catalysts

MDPI

Review

Catalysts for the Selective Oxidation of Methanol

Catherine Brookes [1,2,*,†], Michael Bowker [1,2,†] and Peter P. Wells [2,3,†]

1 Cardiff Catalysis Institute, School of Chemistry, Cardiff University, Main Building, Park Place, Cardiff CF10 3AT, UK; bowkerm@cardiff.ac.uk
2 Rutherford Appleton Laboratory, UK Catalysis Hub, Research Complex at Harwell (RCaH), Harwell, Oxon OX11 0FA, UK; peter.wells@rc-harwell.ac.uk
3 Department of Chemistry, University College London, 20 Gordon Street, London WC1H 0AJ, UK
* Correspondence: catherine.brookes@rc-harwell.ac.uk; Tel.: +44-0-1235-67836
† These authors contributed equally to this work.

Academic Editors: Keith Hohn and Stuart Taylor
Received: 1 April 2016; Accepted: 27 May 2016; Published: 23 June 2016

Abstract: In industry, one of the main catalysts typically employed for the selective oxidation of methanol to formaldehyde is a multi-component oxide containing both bulk $Fe_2(MoO_4)_3$ and excess MoO_3. It is thought that the excess MoO_3 primarily acts to replace any molybdenum lost through sublimation at elevated temperatures, therefore preventing the formation of an unselective Fe_2O_3 phase. With both oxide phases present however, debate has arisen regarding the active component of the catalyst. Work here highlights how catalyst surfaces are significantly different from bulk structures, a difference crucial for catalyst performance. Specifically, Mo has been isolated at the surface as the active surface species. This leaves the role of the Fe in the catalyst enigmatic, with many theories postulated for its requirement. It has been suggested that the supporting Fe molybdate phase enables lattice oxygen transfer to the surface, to help prevent the selectivity loss which would occur in the resulting oxygen deficit environment. To assess this phenomenon in further detail, anaerobic reaction with methanol has been adopted to evaluate the performance of the catalyst under reducing conditions.

Keywords: methanol oxidation; active site; redox; formaldehyde synthesis; model catalysts; surface specificity; XAFS; iron molybdate; spectroscopy; core-shell catalysts

1. Introduction

The selective oxidation of methanol to formaldehyde is a fundamental industrial reaction, reflected by its global demand in excess of 30 million tonnes *per annum* [1]. Formaldehyde stands as the most profitable aldehyde, heavily relied upon due to its diverse and widespread applications including as a building block to the production of dyes, resins, and adhesives.

Since 1931 [2], the most commonly adopted catalyst employed industrially is an iron molybdate based catalyst, $Fe_2(MoO_4)_3$, to which an excess of MoO_3 is added to the chemical composition. This mixed oxide catalyst is considered by many to be a more economical means of effecting partial oxidation of methanol, compared to other oxides and Ag catalysts. Under this approach, formaldehyde yields of 95% are reported, however in order to exploit this process further it is crucial that scientist's gain an understanding of the working catalyst, and the active site/s which dictate the chemistry.

The addition of excess MoO_3 to the catalyst is considered essential. Although the process is operated at relatively low temperatures to discourage over-oxidation of methanol, at these temperatures MoO_3 is shown to sublime from the catalyst as a white residue [3]. This consequently leaves a catalyst Fe rich in nature, which is detrimental to catalyst performance, directing selectivity towards carbon oxide products [4,5]. With excess MoO_3 in the chemical make-up, catalyst lifetimes are prolonged to last between 6 and 12 months.

With both an excess of MoO_3 and stoichiometric $Fe_2(MoO_4)_3$ deemed necessary in the chemical composition, debate has arisen between authors regarding which of these phases dominates as the active species [6–10], or whether indeed there is a synergy between the two [11,12]. MoO_3 is highly regarded for its excellent selectivity to formaldehyde, due to its high capacity to increase oxygen availablity at the catalyst surface. However, whilst MoO_3 may be a highly selective system, the conversion of methanol feedstock is poor. This is a consequence of its low surface area and anisotropic structure [13], which reduces the availability of active sites for the reaction. Conversely, $Fe_2(MoO_4)_3$ is isotropic in nature with an increased surface area, therefore making it a more suitable catalyst choice in terms of activity. Nonetheless, $Fe_2(MoO_4)_3$ does not present an analogous performance to MoO_3 in terms of its' selectivity, unable to compete with the almost 100% selectivity to formaldehyde reported for the single phase oxide [14]. A recent study by Söderhjelm et al. [11] has highlighted that both phases are required for optimized performance, emphasising that the MoO_3 is not simply there to replenish lost Mo. Here they proposed a synergistic effect between MoO_3 and $Fe_2(MoO_4)_3$; implying that the active phase may be Mo-rich, existing as an amorphous layer in octahedral co-ordination at the surface. Each oxide plays its own specific role. Specifically, MoO_3 is believed to enable dissociation of molecular O_2 to atomic oxygen, whilst $Fe_2(MoO_4)_3$ utilises this atomic oxygen to oxidise methanol to formaldehyde. The theory postulated arises from initial studies involving MoS_2/Co_9S_8. Here it was suggested that the promotion of one phase occurs at the junction of the two phases, modifying the electronic density of the catalytic active phase. This is in line with the remote control theory [15], which is applied to catalysts with two oxide phases. One acts as an acceptor phase (in this instance $Fe_2(MoO_4)_3$), whilst the other is the donor (MoO_3). $Fe_2(MoO_4)_3$ enables HC activation, acting independently with limited activity. MoO_3 as the donor phase has a role in providing oxygen activation at a high rate, to spill over and accelerate the overall catalytic cycle. Routray et al. more recently propose a further hypothesis [12]. Work also highlighted a possible synergy between the two oxides. The addition of excess crystalline MoO_3 to the crystalline $Fe_2(MoO_4)_3$ phase significantly increased the overall steady-state catalytic performance toward HCHO formation. The enhanced catalytic performance of the bulk catalyst in the presence of excess MoO_3 was attributed to the formation of third species, a segregated surface MoO_x monolayer. The role of the excess crystalline MoO_3 was identified to replenish the surface MoO_x lost by volatilization during methanol oxidation. Work herein exploits this theory, with the challenging aim to unravel the nature of the active site in commercial $Fe_2(MoO_4)_3$ catalysts, through use of model MoO_x/Fe_2O_3 catalysts. Also questioned is the role of Fe in the catalyst.

2. Mo Segregation

Although the exact nature of the active species in iron molybdate based systems remains unknown, it is now frequently reported [7,10,12,16–20] that Mo surface-segregation readily occurs in iron molybdate systems. XPS studies of bulk iron molybdate have revealed that annealing at 400 °C facilitates the migration of molybdenum to the catalyst surface [21], even when present at low bulk levels. The majority of surface investigations however have exploited electron microscopy studies. Work by Bowker et al. has used aberration corrected scanning transmission electron microscopy (acSTEM) [22], to show that the surface of these catalysts are enriched with Mo. EDX line scans showed a clear dominance of the surface region by Mo, to the detriment of Fe. In support of this, Holmberg et al. [11] have focused on the surface of FeMo catalysts, specifically the origin of the improved catalytic performance of bulk iron molybdate catalysts with extra crystalline MoO_3. Low-energy ion scattering (LEIS) analysis of the outermost surface layer revealed that the molybdate catalysts possessed a monolayer of surface MoO_x species, onto which surface CH_3OH and CH_3O were shown to be present by IR spectroscopy. The enhanced catalytic performance of bulk $Fe_2(MoO_4)_3$ catalysts in the presence of excess MoO_3 was attributed to this surface MoO_x monolayer. HRTEM imaging proved an amorphous surface structure on the edges of the crystals. A similar structure was observed by Gai and Labun [23], when focussing on bulk structures and their reduction. The EDS data showed that the amorphous structure on the fresh catalyst was rich in Mo, whereas for the post

reaction sample there was a lower Mo content. The link between ageing and composition implied that the active material was the amorphous structure at the surface.

In addition to characterization, reactivity data has proved a key tool in providing evidence of Mo segregation [14]. Fe_2O_3 itself is a highly unselective catalyst for methanol oxidation, producing a formate intermediate leading to CO_2 through complete combustion. However, with low loadings of Mo (just 0.25 monolayers present), iron oxide exhibits a significantly different selectivity, apparent by the identification of CO and H_2CO in the reaction profile. The change in selectivity is reflective of the dominance of Mo at the surface. This has also been seen through TPD (Temperature Programmed Desorption) analysis. TPD of Methanol on MoO_3 and $Fe_2(MoO_4)_3$ are remarkably similar (Figures 1 and 2), albeit a slight difference in the ratio of formaldehyde production due to the difference in activity of these two materials. This infers a similar terminating layer in these bulk materials, a surface rich in Mo. Mo has been concluded to be dominant at the surface of iron molybdate based catalysts, existing in its active and selective form, Mo (VI). Mo under this oxidation state is deemed crucial to optimal catalyst performance. Confirmation derives from experiments carried out to determine the activity profile of the other main oxidation state of Mo, which is Mo (IV) [22,24]. During reaction, the active Mo (VI) briefly exists as reduced Mo (IV), which can readily use gas phase oxygen to re-oxidise back to Mo (VI). The identification of the specific conformation of the active site, however, remains elusive.

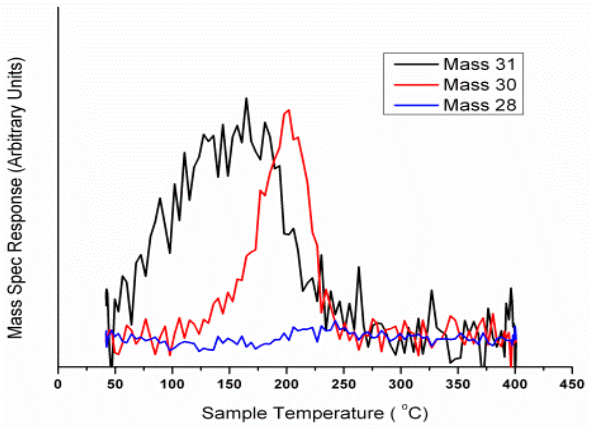

Figure 1. TPD profile for MeOH adsorbed onto the surface of MoO3 For these experiments, MeOH was adsorbed onto the surface of the catalyst, through injection into a flow of He over the catalyst. MeOH was adsorbed to saturation, after which the catalyst was ramped to 400 °C under He, whilst monitoring the products of desorption through mass spectrometry.

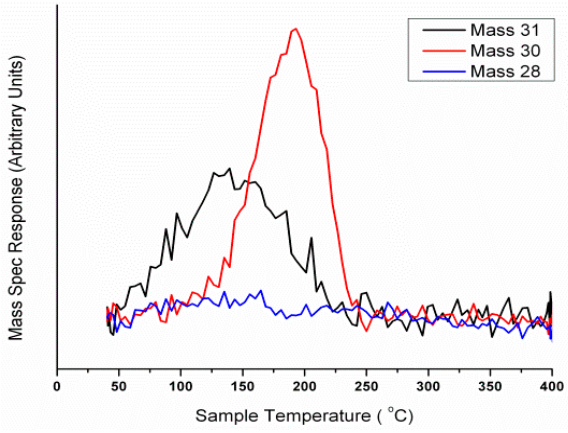

Figure 2. TPD profile for MeOH adsorbed onto the surface of $Fe_2(MoO_4)_3$. Method as in Figure 1.

3. Model Catalysts for Surface Science Investigations

Although the active species in iron molybdate based systems remains unclear, it is however unanimously agreed that the topmost layer of any heterogeneous catalyst is crucial to the efficiency of that material. This paves the way for a more surface science type of approach, utilizing thin layer model catalysts.

The mechanistic understanding obtained from model catalyst studies has become influential in creating better catalysts. The initial drive for a surface science approach to studying heterogeneous catalysts dates back to the pioneering work of Langmuir in the 1910s, in which he studied the adsorption of gases on catalyst surfaces [25]. Since then, surface science studies have been influential in improving catalyst design

Model catalysts have been important for the identification of the stability of Mo at the exterior of Fe containing supports [20]. Surface science experiments with single crystals have shown Mo is stable at the surface of Fe_2O_3 single crystals, even after heating to well above normal calcination temperatures (~400 °C). The driving force for this segregation however, remains unclear.

4. Making XAFS Surface Sensitive

Characterisation of bulk FeMo catalysts has been possible through a number of techniques, most commonly through Raman, FT-IR, DRIFTS, XRD and XPS [14,22,26–29]. The structures of MoO_3 and $Fe_2(MoO_4)_3$ are reasonably well understood, however there still remains some doubt in how they react with methanol, and which phase is predominantly involved in the reaction. There is a requirement to turn to more surface sensitive techniques to probe the uppermost layers in these catalysts. The use of X-ray absorption spectroscopy (XAS) has been the primary focus of our group.

The use of XAS to probe bulk $Fe_2(MoO_4)_3$ has so far been limited in the literature. Due to the significance of the surface layer, XAS as a bulk technique has not been highly considered. There are however a few examples of surface Mo studies [30]. Sarti et al. [31] have investigated the structural and morphological characterization of Mo coatings for high gradient accelerating structures on Al_2O_3. XAS experiments were performed at the Mo K-edge, to determine the chemical status of the Mo atoms. Mo was discovered to exist as a slightly disordered structure at the surface. Hu et al. [32] have also studied the surface structures of supported MoO_3 catalysts by Raman and Mo L-edge XANES. Supported MoO_3 catalysts on TiO_2, Al_2O_3, ZrO_2, and SiO_2, were prepared through incipient-wetness impregnation. At high surface coverages of MoO_3, for TiO_2, the Mo species was shown to form in octahedral coordination, whereas for Al_2O_3 there was a mixture of tetrahedral and octahedral co-ordinated species. On SiO_2 the Mo oxide showed an isolated structure, which resembles a mixed coordination between tetrahedral and octahedral formation.

Most recent work of the author group has turned to studying model materials of the type MoO_x/Fe_2O_3 [7,16,27], in order to gain knowledge into the active surface Mo species. Brookes et al. [16] have confirmed Mo segregation in these core-shell structures, through exploitation of TEM-EDX studies. Inspecting EDX line profiles, Mo was demonstrated to be populated at the surface to the detriment of Fe (Figure 3). Reactivity data supported this, with a stark difference in methanol reactivity between in the absence of Mo (CO_2 and H_2O dominant products) and with Mo present (H_2CO and CO dominant products), inferring the Mo to play a key role in adsorbing the incoming MeOH at surface. Since Mo is present only at the surface, this enables the use of XAFS, which is normally a bulk averaging technique, to be exploited in a surface sensitive approach when tuned to the Mo K-edge.

Initial work involved dosing three monolayers (3ML) of Mo onto the surface of Fe_2O_3, since this gave good sensitivity for spectroscopy techniques, most importantly for XANES. The interpretation of the Mo XANES spectra included the assignment of the pre-edge peak at ca. 19,995 eV, and the peak at 20,010 eV. The first is attributed to the dipole-forbidden/quadrupole-allowed 1s–4d transition [33], associated primarily with tetrahedral geometry, but it is also present, albeit weaker, in structures with distorted octahedral geometry. The peak at 20,010 eV is assigned to the dipole-allowed 1s–5p transition and is a characteristic feature of Mo species with octahedral/distorted octahedral geometry.

The XANES spectrum of the dried 3ML MoO_x/Fe_2O_3 sample (120 °C) is shown in Figure 4. Comparing this with bulk MoO_3 (Figure 4 also), it was found that the dried phase showed a much weaker pre-edge feature at 19,995 eV, associated with the distorted octahedral structure of this initial phase. Differences were also evident in the intensity of the peak at 20,010 eV.

EXAFS interpretation (Figures 5 and 6) was also assessed to clarify differences between the dried phase and commercial MoO_3. The k^2-weighted χ data showed a similar phasing and amplitude for the two samples at values of low k. However, the discrepancy at higher k inferred a lack of long range order for the dried sample, also supported by the radial distribution plot which showed an absence of a secondary coordination shell (Mo–Mo) as seen for MoO_3 (Figure 6). This was indicative of the fewer high Z neighbours associated with the dried phase, and its overall lack of dimensionality. For this reason the dried phase was referred to as MoO_x, since it could not be indexed to any known phase of Mo.

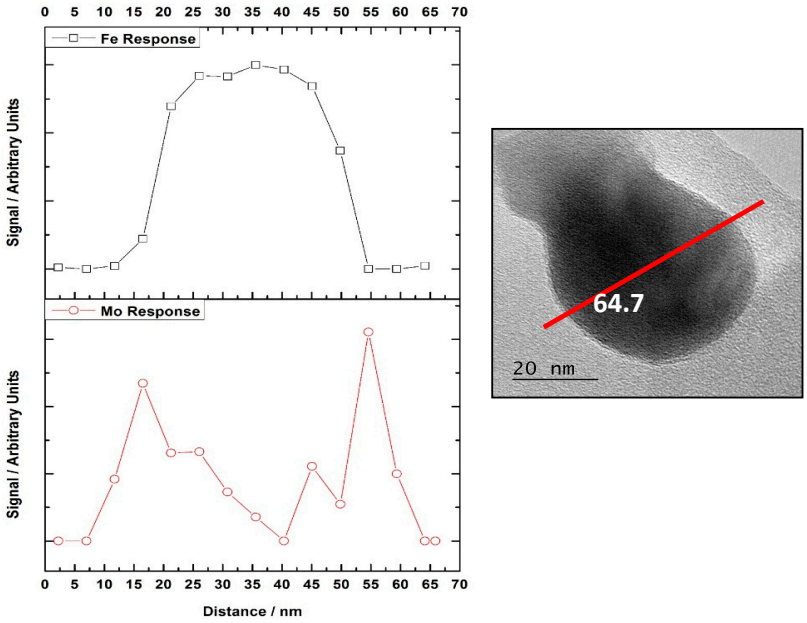

Figure 3. TEM image of a particle from 3ML MoO_x/Fe_2O_3 after a calcination at 500 °C with accompanying EDX line scan (**right**). Image adapted from C. Brookes et al., *ACS Catal.*, 2014, *4* (1), pp. 243–250 [16].

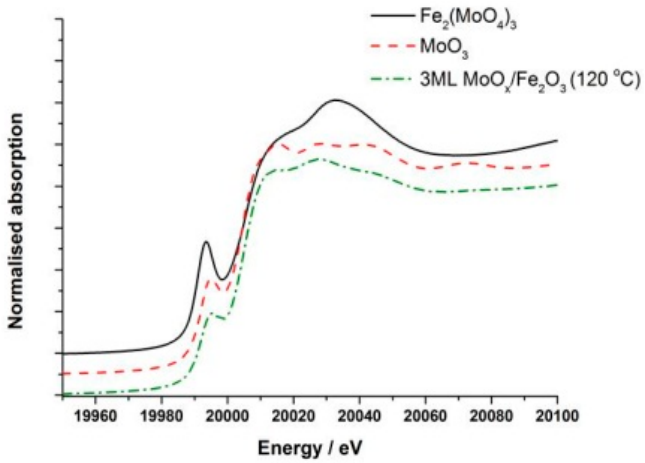

Figure 4. Normalised XANES spectra of dried 3ML MoO_x/Fe_2O_3 (120 °C), MoO_3, and $Fe_2(MoO_4)_3$; Image adapted from C. Brookes et al. *ACS Catal.*, **2014**, *4* (1), pp. 243–250 [16].

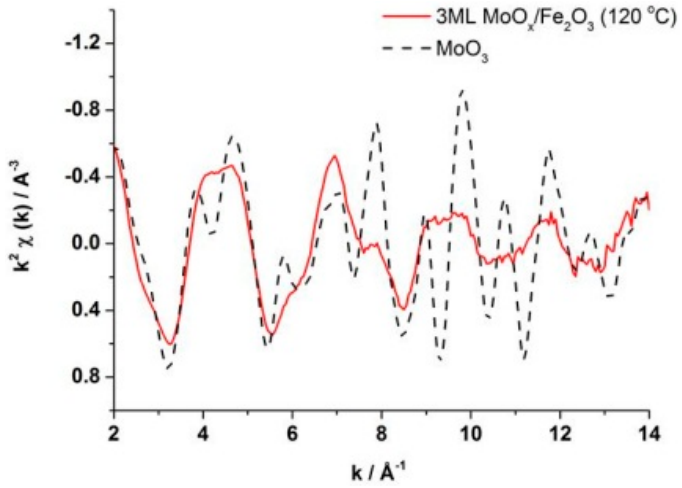

Figure 5. k2-weighted data and (6) Fourier transform (non phase-corrected) for 3ML MoO_x/Fe_2O_3 (120 °C) and MoO_3. Image adapted from C. Brookes et al. *ACS Catal.*, **2014**, *4* (1), pp. 243–250 [16].

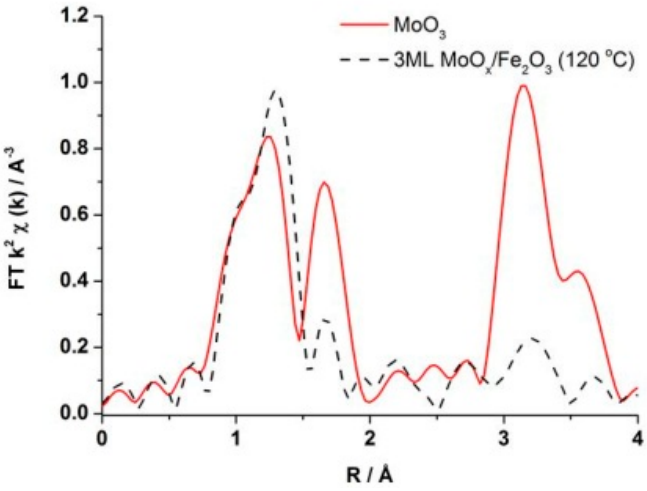

Figure 6. Fourier transform (non phase-corrected) for 3ML MoO_x/Fe_2O_3 (120 °C) and MoO_3. Image adapted from C. Brookes et al. *ACS Catal.*, **2014**, *4* (1), pp. 243–250 [16].

The effect of annealing temperature on the nature of the Mo within these samples was also investigated. Assessing through XANES (Figure 7), analysis showed there were no changes observed between the dried material and that calcined to 300 °C. The k^2-weighted χ spectrum of the 400 °C annealed sample however, indicated that the sample began to show features associated with MoO_3 phase formation. With further annealing to 500 °C, large amounts of Mo began to be incorporated into a tetrahedral $Fe_2(MoO_4)_3$ phase, depicted through a distinctive rise in the pre-edge feature at 19,995 keV (Figure 7).

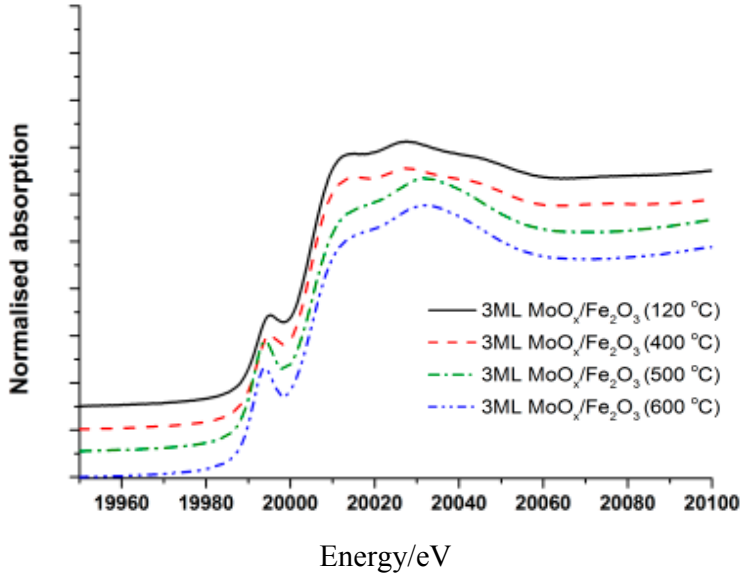

Figure 7. XANES spectra of 3ML MoO_x/Fe_2O_3 catalysts annealed to different temperatures. Image adapted from C. Brookes et al., *ACS Catal.*, 2014, *4* (1), pp. 243–250 [16].

Table 1 details the phase compositions calculated through linear combination fittings (LCF's) for various anneal temperatures between 120 and 600 °C. LCF's were performed using the initial dried at 120 °C phase (MoO_x), MoO_3 and $Fe_2(MoO_4)_3$ as references. For a theoretical understanding, Figure 8 displays a simplified schematic with the associated summary of these initial findings. It is shown that at temperatures above 400 °C, most of the Mo converted to $Fe_2(MoO_4)_3$, with Mo from the surface reacting with the Fe_2O_3 core to form a tetrahedral structure. Below this temperature, nanocrystalline MoO_3 was present in the sample, forming at 400 °C. Crucially, Raman was only able to prove the existence of these two Mo oxide phases (Figure 9), being MoO_3 and $Fe_2(MoO_4)_3$, whereas XAFS revealed a third component, MoO_x, present under all heat treatments employed. This is much in line with the opinions of Routray et al. [12]. Interestingly, despite the differing Mo oxide phases between the samples dried at 120 °C, 400 and 500 °C, all of these catalysts showed a similar activity (Figure 10, reactivity dominated by H_2CO and CO formation for all catalysts) [16]. For this reason, the octahedral MoO_x surface layer present for all temperatures between 120 and 600 °C, was deemed the active and selective overlayer for formaldehyde synthesis. The material was both activated and improved in selectivity due to the dominance of the methoxy species on this Mo-doped material, in contrast to the stable formate which is seen to form on Fe_2O_3 [4].

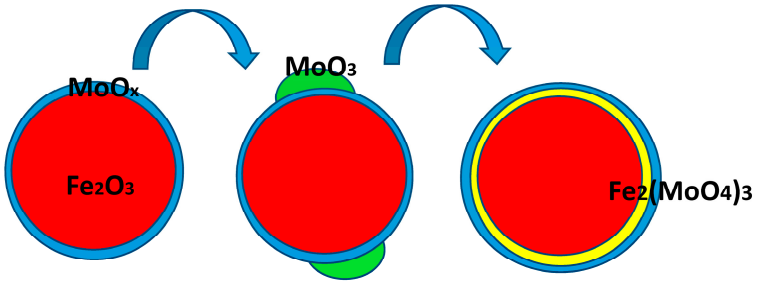

Figure 8. The evolution of the surface structure of the 3ML catalyst, as a function of annealing temperature. (**Left**) Structure at 120 °C. Fe_2O_3 (red), with an amorphous layer of MoO_x (blue); (**Middle**) Structure at 400 °C. MoO_3 nanocrystallites (green) at the surface of the catalysts, and the surface of MoO_x present; (**Right**) Structure at 500 °C, MoO_3 nanoparticles have converted to $Fe_2(MoO_4)_3$ (yellow), which is an underlayer to the topmost and active layer O_h MoO_x.

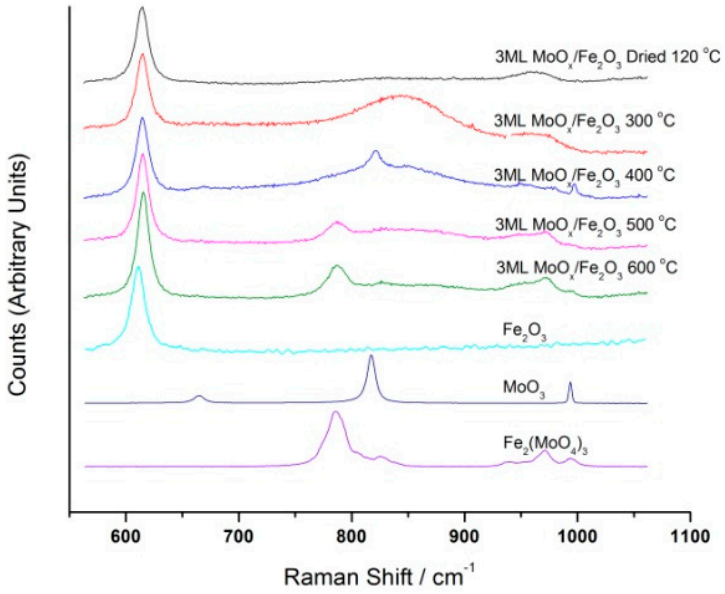

Figure 9. Raman spectra of 3ML MoO_x/Fe_2O_3 for dried 120 °C, 300, 400, 500, 600 °C and their reference spectra Fe_2O_3, MoO_3 and $Fe_2(MoO_4)_3$. Image adapted from C. Brookes et al. *ACS Catal.*, 2014, *4* (1), pp. 243–250 [16].

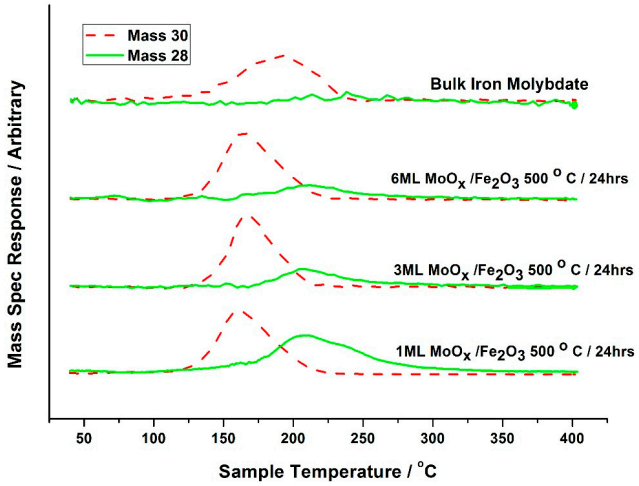

Figure 10. TPD data obtained for 1, 3 and 6ML's MoO_x/Fe_2O_3, after calcining at 500 °C for 24 h and dosing with methanol at ambient temperature, with noticeable reduction in CO production. Subtractions have been made for the various cracking fragmentations of each product. All monolayer coverages show a very similar reactivity profile, albeit a slight different in the ratio of H_2CO:CO formation. Image adapted from C. Brookes et al., *J. Phys. Chem. C*, 2014, *118* (45), pp. 26155–26161 [7].

Table 1. XANES LCF fittings for 3ML MoO_x/Fe_2O_3. Fittings were performed using the initial dried 3ML MoO_x/Fe_2O_3 material, $Fe_2(MoO_4)_3$ produced in-house, and commercial MoO_3.

Sample	Reference Standards		
	MoO_3 (%)	**MoO_x/Fe_2O_3 (%)**	**$Fe_2(MoO_4)_3$ (%)**
3ML MoO_x/Fe_2O_3 (400 °C) XANES fit	14	86	-
3ML MoO_x/Fe_2O_3 (400 °C) chi fit	25	75	-
3ML MoO_x/Fe_2O_3 (500 °C) XANES fit	-	38	62
3ML MoO_x/Fe_2O_3 (600 °C) XANES fit	-	40	60

To extend from this study, further monolayer coverages were investigated by Brookes et al. [7]. It was discovered that just one monolayer of Mo on iron oxide alone was successful in producing formaldehyde, albeit with a slight increase in CO production due to the inability to form a complete monolayer coverage over the Fe_2O_3 core. This lack of coverage subsequently leaves a surface with exposed Fe sites, which are detailed by Bowker et al. to be responsible for CO production through direct methanol dehydrogenation [8,27]. Fe_2O_3 coverage is considered crucial in dictating the selectivity of the reaction. Work by Huang et al. [34] has investigated the influence of thermal spreading of MoO_3 on the surface of Fe_2O_3, and the solid-state reaction that produces $Fe_2(MoO_4)_3$ during heat treatment. XPS, SEM and Mössbauer spectroscopy were used to characterize the evolution of the surface. It was found that a small amount of MoO_3 can be dispersed onto the surface of Fe_2O_3 relatively easily by simple grinding of the two oxides. In addition, the thermal spreading of MoO_3 is facilitated at around 400 °C. Further thermal spreading and the solid-state reaction yield a shell of $Fe_2(MoO_4)_3$ encapsulating the remaining Fe_2O_3 grains, but a small amount of MoO_3 remains on the external surface of the resulting $Fe_2(MoO_4)_3$ shell.

In support of this, Brookes et al. [16] have demonstrated the benefits of calcination time, comparing the effects of both a 2 and 24 h treatment on various monolayer catalysts of MoO_x/Fe_2O_3 calcined at 500 °C. Catalysts across the monolayer range all demonstrated a significantly improved selectivity towards formaldehyde with a longer calcination time, with the 1ML catalyst showing the most significant improvement. For 1ML dosed, a clear production of CO_2 was observed though TPD analysis after a two hour calcination. This is in stark contrast to the performance after a 24 h heat treatment, which only disclosed CO and H_2CO to desorb from the surface. This is reflective of the improved spread of the Mo at the surface, although no characterization has been performed to support this. The work highlighted the importance of investigating the evolution of the surface state during the preparation of a catalyst.

With an ongoing interest in this active amorphous overlayer of Mo, focus turned to studying the 1ML MoO_x/Fe_2O_3 catalyst more thoroughly through spectroscopy techniques [7]. Both Raman and XANES data revealed a uniform absorption spectrum across the calcination range for 1ML MoO_x/Fe_2O_3 treated between 120 C and 600 °C (Figure 11), also analogous to the dried 3ML MoO_x/Fe_2O_3 phase previously discussed. It was therefore recognized that for a monolayer (or sub-monolayer) amount of a species (labelled MoO_x), the molybdenum remains segregated at the surface of the Fe_2O_3, with complete O_h geometry under all calcination conditions (Figure 11).

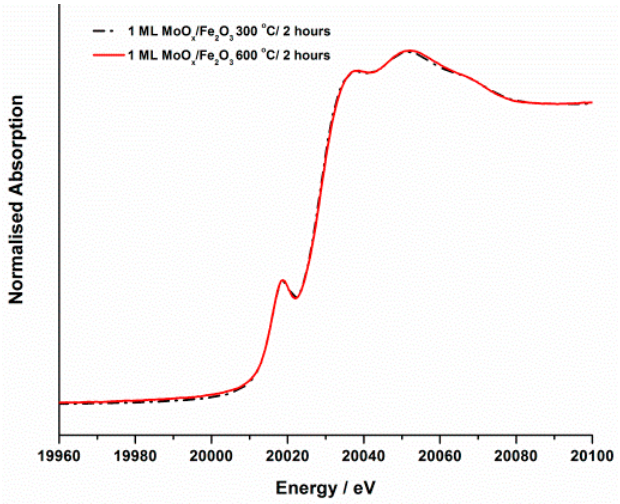

Figure 11. Normalised XANES spectra of 1ML MoO_3/Fe_2O_3 catalysts annealed to 300 and 600 °C. Spectra are identical across the calcination range. Image adapted from C. Brookes et al., *J. Phys. Chem. C*, 2014, *118* (45), pp. 26155–26161 [7].

A detailed EXAFS analysis was able to assess the local structure of this amorphous O_h overlayer in more detail. The non-phase-corrected Fourier transform of the k^2-weighted EXAFS data for the 1ML MoO_x/Fe_2O_3 sample annealed at 500 °C for 24 h is detailed in Figure 12, with obtained EXAFS parameters in Table 2. EXAFS data exposed that the O_h Mo units are bound to the Fe_2O_3 surface with through a Mo–Fe interaction. The primary Mo O_h environment was dominated by oxygen neighbors, with the major contribution at low values of R in the Fourier transform. This was ascribed to a short Mo–O (distance = 1.74 Å) scattering path (Table 2). Also present was a longer Mo–O scattering path (distance = 1.95 Å), but with less impact on the EXAFS data as a consequence of the large disorder associated with it. Further out in R space (after 2 Å), Mo–Fe scattering paths dominated, albeit weak in intensity due to their out of phase nature (See imaginary part, Figure 12). Computational studies performed later in collaboration with David Mora Fonz of UCL, were in agreement with the results obtained through EXAFS [7]. Modelling was undertaken to determine the nature of the preferred adsorption site on the most stable surface (0001) of α-Fe_2O_3. The favoured adsorption site was indicated to be where the Mo would have three Fe neighbors at approximately 3 Å, in addition to one shorter distance Fe neighbor. Figure 13 represents these findings [7].

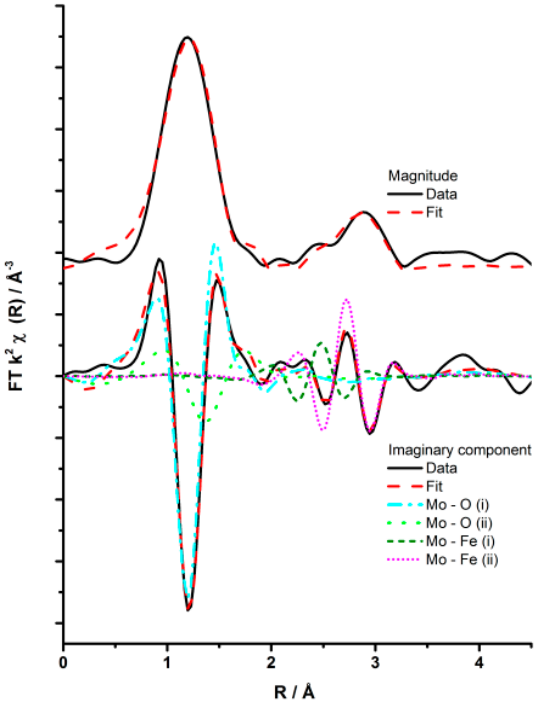

Figure 12. Magnitude and imaginary component of the k^2-weighted Fourier transform (non phase-corrected) for the EXAFS data of the 1ML MoO_x/Fe_2O_3 catalyst calcined to 500 °C/24 h. Associated scattering paths are included for the imaginary component. Image adapted from C. Brookes et al., *J. Phys. Chem. C*, 2014, *118* (45), pp. 26155–26161 [7].

Table 2. EXAFS fitting parameters for the 1ML MoO_x/Fe_2O_3 catalyst calcined to 500 °C Fitting parameters: $S_0{}^2 = 0.82$ as deduced by MoO_3 standard: Fit range $2.6 < k < 9.7$, $1 < R < 3.5$; # of independent points = 11. Where N = Co-ordination number, R = Bond distance/Å of the Absorber-Scatterer, $2\sigma^2$ = Mean squared disorder, E_f = Eo, R_{Factor} = A statistic of the fit.

Abs. Sc.	*N*	*R*/Å	$2\sigma^2$/Å^2	E_f/eV	R_{factor}
Mo–O	3 (fixed)	1.74 (2)	0.006 (1)	7 (3)	0.005
Mo–O	3 (fixed)	1.95 (6)	0.03 (1)	-	-
Mo–Fe	1 (fixed)	2.85 (4)	0.009 (6)	-	-
Mo–Fe	3 (fixed)	3.10 (3)	0.009 (3)	-	-

In conclusion so far, the data have indicated a stable amorphous O_h overlayer of Mo at the surface of Fe_2O_3, present for a range of monolayer coverages and calcination temperatures. Catalyst screening studies revealed a comparable performance for all levels of Mo dosed onto Fe_2O_3. Most significantly, catalysts with just one monolayer coverage of molybdenum on Fe_2O_3 resulted in a very selective catalyst for methanol oxidation to formaldehyde. It was proposed by Brookes et al. [16] that this common surface overlayer present for all such catalysts, is also the active overlayer in bulk ferric molybdate catalysts of the type used industrially.

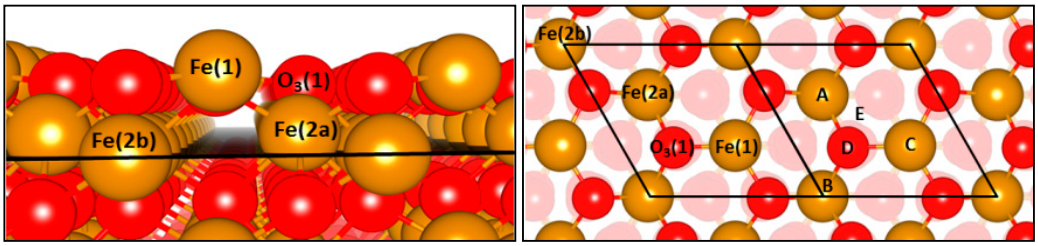

Figure 13. (**Left**) side view of the α-Fe_2O_3 (0001) surface. The drawn plane marks the position of the semi-transparent oxygen ions; Brown sphere = Fe, Red sphere = O, (**Right**) view along the hexagonal axis of the α-Fe_2O_3 (0001) surface. Different initial adsorption sites (from A to E) for the MoO_3 unit are shown; the rhombi represent the surface unit cell. Image adapted from *J. Phys. Chem. C*, 2014, *118* (45), pp. 26155–26161 [7].

5. Initial Investigations into the Mechanism and Reaction Site of Methanol on FeMo Based Catalysts

In highlighting the use of model MoO_x/Fe_2O_3 catalysts to gain knowledge into the possible surface terminations in bulk FeMo systems, the work of Brookes et al. [35] next exploited in situ characterization, specifically to address the reaction mechanisms occurring with methanol. Although widely valued for its efficacy in the reaction, there is a surprising lack of knowledge regarding the catalyst surface layer in $Fe_2(MoO_4)_3$, and more importantly how it reacts with the incoming methanol reactant under high pressure conditions. This has been a topic of great interest, with many authors able to identify the phases which are formed through reduction and regeneration of the catalyst [3,36–38], but unable to designate these intermediate phases to a defined reaction mechanism.

The mechanism of methanol adsorption and reaction on the surface of FeMo based catalysts has been extensively researched, with the majority of authors recognizing that the Mars-Van Krevelen mechanism applies [12,39]. Under this mechanism, methanol oxidation employs surface lattice oxygen [40], inducing a temporary partial reduction of the surface to Mo (IV).

The reduction mechanism has been reported to occur as follows, resulting in a mixed phase catalyst [38]:

$$CH_3OH + Fe_2(MoO_4)_3 \rightarrow 2\beta - FeMoO_4 + MoO_3 + HCHO + H_2O \quad (1)$$

This is then counteracted by a quick regeneration through gas phase oxygen to Mo (VI).

$$2FeMoO_4 + MoO_3 + 1/2O_2 \rightarrow Fe_2(MoO_4)_3 \quad (2)$$

House et al. [22,41] have exploited TPD and pulsed flow studies to investigate this reduction phenomenon in more detail. The reaction and reduction of iron molybdate (Mo:Fe = 2.2:1) with methanol feedstock under anaerobic conditions was adopted. The first pulse of methanol demonstrated comparable conversion and selectivity to formaldehyde, as would be seen under aerobic conditions. This indicated that gas phase oxygen is not directly required in the reaction, but is merely there to re-oxidise the surface for continued use, again supporting the MVK mechanism. With further reduction at low temperatures, the catalyst performance diminished, reflecting the significant loss of oxygen from

the catalyst surface. However, contrary to this, as the temperature is elevated above 250 °C, the catalyst was able to reinstate its previous activity, as bulk oxygen migrates to the surface at a higher rate to enable the production of formaldehyde. With loss of bulk oxygen, further oxide phases inevitably formed, with XRD evidencing α-$FeMoO_4$, MoO_2, and Mo_4O_{11}. The study was informative not only in providing information regarding these reduced phases, but also in preliminary investigating the mechanisms occurring at the surface.

TPR studies performed by Zhang et al. [42] on $Fe_2(MoO_4)_3$ with excess MoO_3 highlighted the transformation of $Fe_2(MoO_4)_3$ to β-$FeMoO_4$ and Mo_4O_{11}, MoO_3 to MoO_2 and β-$FeMoO_4$ to $Fe_2Mo_3O_8$ and Fe_3O_4. Beale et al. also describe their related work [38], specifically studying $Fe_2(MoO_4)_3$ using in situ WAXS, XANES and UV- Vis. Under reducing conditions, they observed the reduction to produce β-$FeMoO_4$ and MoO_3, which can further reduce to MoO_2. It is thought from previous literature studies of methanol oxidation over bulk $Fe_2(MoO_4)_3$, that the formation of reduced α-$FeMoO_4$ occurs at lower temperatures, whilst β-$FeMoO_4$ dominates at higher temperatures above 310 °C [43].

Due to its dominance of the surface layer of highly selective ferric molybdate catalysts, focus has turned to studying methanol reaction on Mo surfaces, specifically MoO_3. The crystallographic planes in MoO_3 have been resolved by electron diffraction as the apical (001 + 101), side (100) and basal (010) planes. The basal (010) plane was found to possess the lowest free energy, lying parallel to the double layer. Ab initio quantum mechanical calculations performed by Allison et al. [44] supported a multistep mechanism involving reaction of methanol with dual-dioxo catalytic sites. Since these dual sites were shown to exist on the (010) face of MoO_3 (Figure 14), this face was deemed as the reactive site [45]. However, this is not unanimously agreed, with several authors revealing that the (010) plane exhibits especially low saturation, and any methanol adsorption occurring does not contribute to formaldehyde production. The role of this face is still under investigation for selective methanol oxidation [14,45].

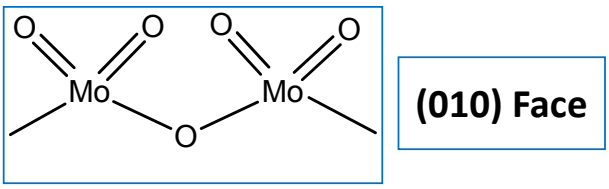

Figure 14. Proposed dual-dioxo catalytic sites on the 010 face of α-MoO_3.

It has since been proposed that methanol adsorption occurs at the edge and defect sites of α-MoO_3, since the uptake of methanol correlates accordingly with the number of active centres on these sites. Edge planes are formed by the bond cleavage perpendicular to the MoO_3 double-layers [46], exposing co-ordinatively unsaturated molybdenum onto which adsorption can occur [47]. Non (010) faces possess the required dual acid-base sites, as outlined in Figure 15. Pre-treatment of the surface with pyridine has shown to inhibit methanol oxidation due to poisoning of the MoO_3 surface. This implies Lewis acid sites, as proposed by Tatibouet et al. [47]. The Lewis acid character revealed by these adsorption studies [48], facilitates substrate interactions.

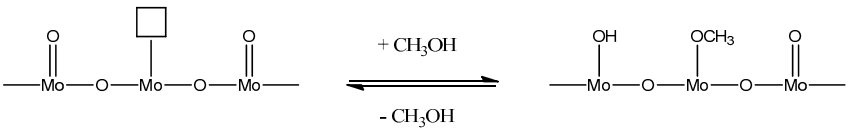

Figure 15. Dissociative chemisorption of methanol on α-MoO_3 [49]. The dual acid-base sites are formed from an unsaturated metal cation (O–Mo–O), and adjacent terminal oxygen (Mo = O) [47]. Methanol can dissociatively chemisorb at these dual sites. The unsaturated Mo atom performs as a Lewis acid centre, acting as the adsorption site for a methoxy intermediate. The basic M = O site abstracts a proton simultaneously to form a hydroxyl. Both intermediates have been evidenced through IR studies [50,51].

The steps which follow the methoxy adsorption, are dependent on the oxidation state of the Mo active centre. If Mo exists as active and selective Mo (VI), the reaction proceeds via scission of the C-H bond, considered to be the rate-determining step. The process yields formaldehyde and a proton, which reacts with lattice oxygen to form a second hydroxide, which proceeds to be lost as water under oxidative conditions [52]. If the oxygen level is insufficient, the produced hydrogen will be introduced into the surface, creating a surface bronze denoted H_xMoO_3. With even further reduction, loss of H occurs with subsequent MoO_2 formation, a known reduced state of MoO_3. The reactivity of iron molybdate is comparable to that of the pure α-MoO_3 in terms of selectivity [22], however, the activity of this mixed phase oxide supersedes that of MoO_3, due to the greater number of exposed catalytic active sites present for isotropic $Fe_2(MoO_4)_3$ than for anisotropic MoO_3. Only the edge sites for MoO_3 can carry out the catalysis, whereas all the exposed planes in $Fe_2(MoO_4)_3$ can dissociatively chemisorb CH_3OH as well as oxidise methanol to formaldehyde.

It is agreed that during the reaction, partial surface reduction occurs, followed by a very rapid regeneration using gas phase oxygen. It could be that Mo (IV) exists temporarily, agreeing with the initial mechanisms of Bowker et al., however, it has not been possible to isolate this species under normal oxidative reaction conditions.

Attempts have been made by our group to explore the nature of Mo during the *oxidative* reaction with methanol [35]. In situ isothermal reaction studies were performed under transmission mode XAFS coupled with mass spectrometry analysis, whilst maintaining the temperature at 250 °C. During formaldehyde production (Mass 30, Figures 16 and 17), no obvious changes were observed in the Mo speciation, inferred by the constant pre-edge position, and maintained T_d co-ordination throughout. With a sustained Mo environment, this allowed for continued production of formaldehyde, as revealed by the mass spectrometer data collected online during the experiment (Figure 17). Previous studies have identified that surface oxygen is consumed in the reaction [7,16]. It is therefore shown from these oxidative studies that any removal of surface oxygen and temporary Mo reduction is difficult to probe, due to the rapid re-oxidation by gas phase oxygen to maintain the catalyst in its desired Mo (VI) state. It could be that Mo (IV) exists momentarily under reactive conditions, but is unable to be seen due to the time scale of these studies. This has proved a challenge for many researchers [24,45].

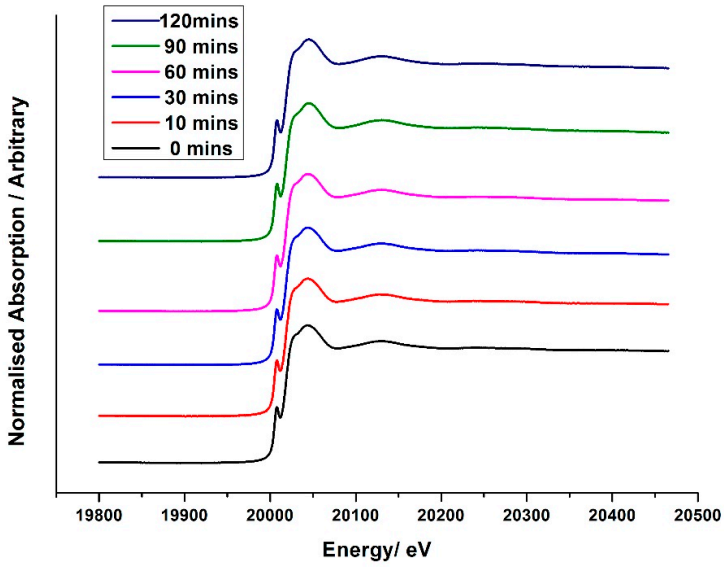

Figure 16. XANES data over a 120 min period for 6ML MoO_x/Fe_2O_3 when reacted isothermally at 250 °C under a continuous flow of $MeOH/O_2$.

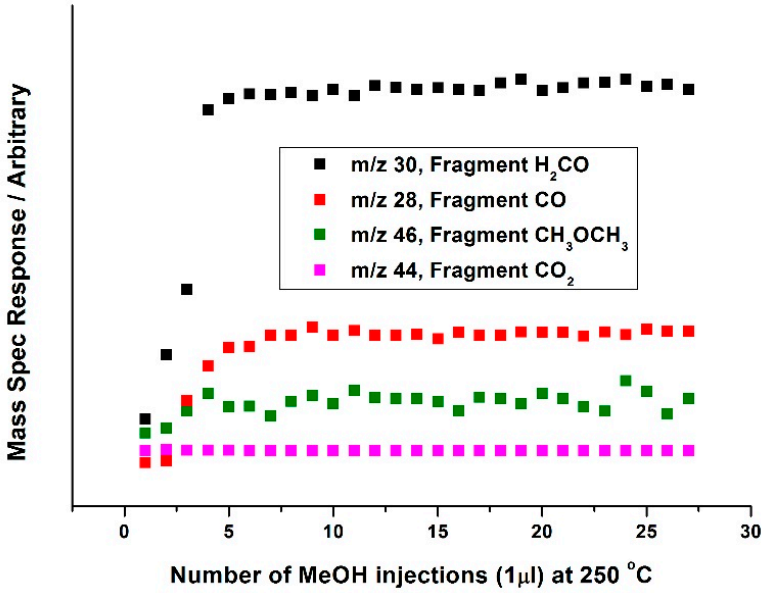

Figure 17. Online mass spectrometry data for experiment of Figure 16. Image adapted from C. Brookes et al., *Catal. Sci. Technol.*, **2016**, 6, 722 [35].

Other authors have exploited alternative approaches to investigating the mechanisms on Mo dominated catalysts.

Bowker et al. [22] have focussed the role of Mo in the selective oxidation of methanol, proposing the terminating Mo = O as an initial single adsorption site for methanol oxidation (Figure 18) [22]. The majority of authors also identify this Mo = O site as a possible dehydrogenation centre for the mild oxidation [7,22,37,47,49]. Trifiro et al. [53] have long maintained the opinion that Mo = O double bonds are essential in oxidation catalysts, with dioxo centres at the core of the reactivity due to their ability to extract both hydrogens from methanol. During the reaction proposed by Bowker et al., the active Mo (VI) reduces to Mo (IV), which can readily use lattice or gas phase oxygen to re-oxidise back to Mo^{6+} Confirmation of this derives from experiments carried out to determine the activity profile of the other main oxidation state of Mo, which is Mo (IV). From experimental observations the scheme was proposed as:

1. An acid-base type reaction occurs at the terminal Mo = O site, resulting in methoxy and OH formation (g = gas phase, a = adsorbed species). The terminal oxygen is deemed the most stable site for hydrogen adsorption.

$$CH_3OH_g + O_t \rightarrow CH_3O_a + OH_a \quad (3)$$

2. Attack of the bridging oxygen on the adsorbed methoxy yields adsorbed formaldehyde and a hydroxyl. This C-H abstraction on methoxy occurs at much higher temperature, and is deemed as the rate-determining step in formaldehyde formation. It is presumed that the step involves bridging oxygen, since when Fe is present at the surface, high selectivity to CO occurs due to the changed bonding energy of the Mo-O-Fe bridging oxygen which dehydrogenates the methoxy intermediate.

$$CH_3O_a + O_b \rightarrow H_2CO_g + OH_a \quad (4)$$

3. OH recombination occurs to yield H_2O from the catalyst [52]. The anion vacancy is re-oxidised from the bulk (anaerobic) or gas phase (aerobic) oxygen.

$$2OH_a \rightarrow H_2O_g + O_s + V_s \quad (5)$$

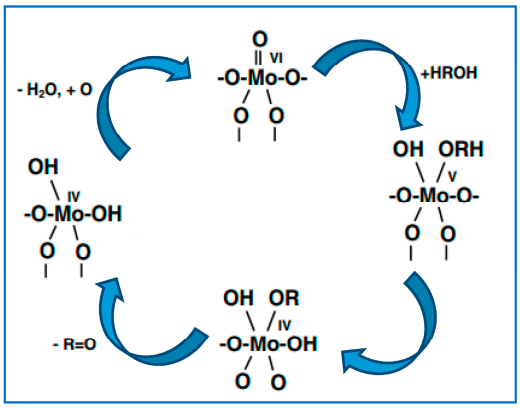

Figure 18. The oxidative dehydrogenation of methanol on molybdenite catalysts as proposed by Bowker et al. [22].

Once formed, formaldehyde can be further oxidised to CO or CO_2. However, the high selectivity of α-MoO_3 is derived from the presence of undissociated methanol and water blocking the adsorption sites, which retards this further oxidation.

A recent paper from our research team reports a simple quantative model to describe the behavior of bi-cationic systems [36], comparing selectivity as a function of Mo loading on Fe_2O_3 (Figures 19 and 20). Surface doped materials are commended for their use in learning about the active configuration and its relationship to high selectivity. It was found that product distribution was highly dominated by the distribution of dual and single sites of the two species (Mo and Fe) at the surface. Mo is highly selectivity on its own to formaldehyde, and is proposed to be present in commercial catalysts as an active Mo monolayer on top of ferric molybdate. Product yield was measured from iron oxide, through to the stoichiometric catalyst, $Fe_2(MoO_4)_3$, considering various Mo doping levels. CO_2 was shown to be dominant at high Fe levels, while H_2CO prevailed for low Fe content. However, over a wide range of the intermediate concentrations, CO was the primary product (Figure 19). It was postulated that double sites are important for the selective reaction. For formaldehyde production, it was concluded that two Mo sites are required, whilst double Fe sites promote combustion on iron oxide via formate adsorption. Where CO was the dominant product, a different active site was proposed, requiring only one cation to be involved in the rate determining step. This appeared to show the general trend of behaviour observed.

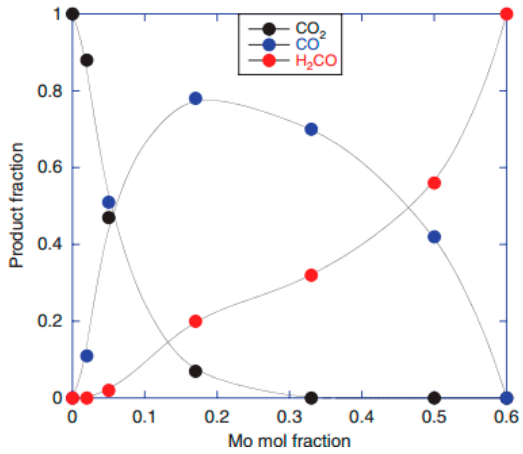

Figure 19. The yields of the three main products of methanol oxidation seen in TPD, as a function of the amount of Mo in the catalyst. A mole fraction of 0.6 corresponds with the stoichiometric materials $Fe_2(MoO_4)_3$. Image adapted from *Catal. Struct. React.*, **2015**,*1*, 95–100 [36].

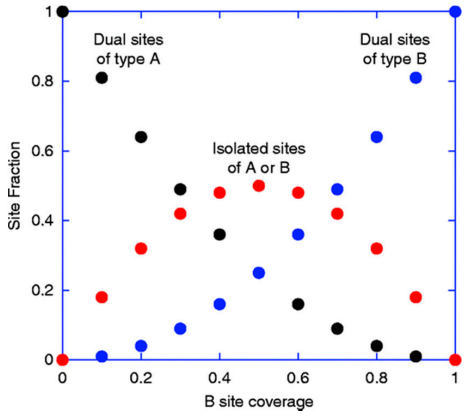

Figure 20. The variation of dual sites and single sites as a function of coverage of type B on the surface. Image adapted from M. Bowker et al., *Catal. Struct. React.*, **2015**,*1*, 95–100 [36].

DRIFTS studies on 6ML (monolayers) MoO_x/Fe_2O_3 calcined at 600 °C, have been carried out by the authors of this review, in support of this theory (Figure 21). Studying model catalysts produced in this way paves the way for a surface analysis approach, whilst also producing catalysts with higher surface areas for maximised infrared signal. Upon dosing with MeOH at room temperature, the formation of two methanol related surface species. The first species exists as a non-dissociatively adsorbed O-H group of methanol, appearing at 3100–3500 cm^{-1} with a second species is observed as pair of bands at ~2955 and 2847 cm^{-1} which can be indexed to the stretch and the first overtone of the symmetric bend of methanol CH_3, respectively [54]. By 100 °C, the DRIFTS spectrum (Figure 21) could also distinguish the bands of methoxy on moderately Lewis-acidic oxides (2933 & 2835 cm^{-1}), differentiating them from the C-H vibrations of undissociated methanol on acidic surfaces at this temperature (2959/2854 cm^{-1}). It should be noted, whilst molecular methanol remains the dominant surface species at low temperature, methoxy dominates at higher temperatures, shown through the maintained intensity of methoxy compared to the loss of related MeOH bands. This would reflect the stronger surface interactions of the methoxy. All associated bands diminished by 200 °C, as reactants subsequently form products.

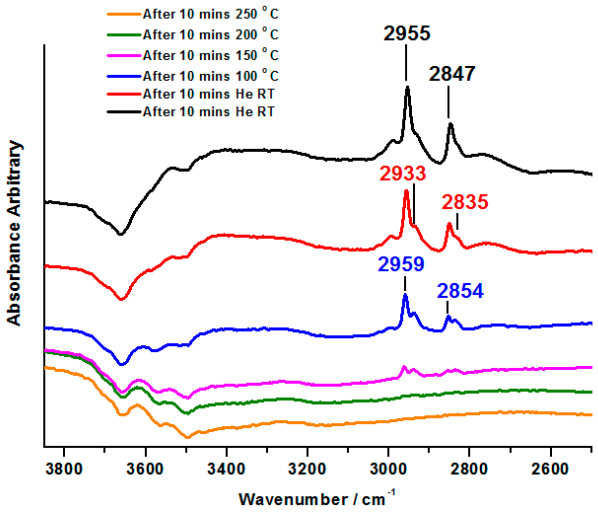

Figure 21. In situ DRIFTS spectra for 6ML MoO_x/Fe_2O_3 under TPD of MeOH/He. The catalyst surface was saturated with MeOH pulses under He at room temperature, and two spectra were then taken with one 10 min after the other (black and red curves). The temperature was then raised to 400 °C, monitoring the reaction products through TPD with simultaneous DRIFTS analysis of the surface species.

6. In Situ Investigations under MeOH/He to Provide Insights into the Reaction Mechanisms under Methanol

Due to the difficulty in probing the active site under oxidative conditions, an alternative approach has been advocated amongst the group of Brookes et al. [35], exploiting their core-shell structures of Mo on Fe_2O_3 under MeOH/He. Reacting anaerobically enforced a reduction of the surface, which could be analogous to the structural changes occurring momentarily under reaction with MeOH under aerobic conditions. Specifically studying core-shell MoO_x/Fe_2O_3 catalysts enabled the use of in situ XAFS as a surface sensitive analysis tool, exclusively probing the active topmost layers, without the added complication of secondary phases such as MoO_2 and β-$FeMoO_4$, which we are shown to be produced during the reduction of bulk $Fe_2(MoO_4)_3$ [42,55].

Figure 22 details the extent of reduction as a function of temperature for 1, 3 and 6 monolayer loadings of Mo on Fe_2O_3, acquired through XANES analysis. Since it was not possible to source appropriate references to perform satisfactory LCA, results were ascertained through observing the move in edge position between Mo (VI) from the original post reduced catalyst, to Mo (IV) referenced from MoO_2, a known reduced state of $Fe_2(MoO_4)_3$,. Observed was an edge shift of approximately 70% towards Mo (IV) for all coverages, implying MoO_2 itself did not form (Figure 23). Further characterization through Raman and XRD was also unable to establish isolated MoO_2, as is the case for bulk $Fe_2(MoO_4)_3$.

To elucidate this reduction process further, EXAFS analysis was influential. The end state k^2-weighted Fourier transform data for the reduced samples of the 1 and 6ML MoO_x/Fe_2O_3 catalysts are shown in Figure 24. The obtained fits were comprised of five scattering paths; one Mo–Mo, 2 Mo–O and 2 Mo–M, where M = Fe or Mo. Two oxygen scattering paths featured at 1.78 and 2.02 Å, indicative of reduced forms of Mo, as well as the distorted nature of the Mo octahedra. Significantly, all monolayers displayed a strong contribution from an Mo–Mo distance at 2.6 Å (Table 3). Literature assigns this to a bonded distance indicating a Mo (V) dimer or Mo (IV) trimer [44]. This bond distance is different from that in MoO_2, which has a shorter distance of 2.5 Å, and with a reduced average co-ordination number.

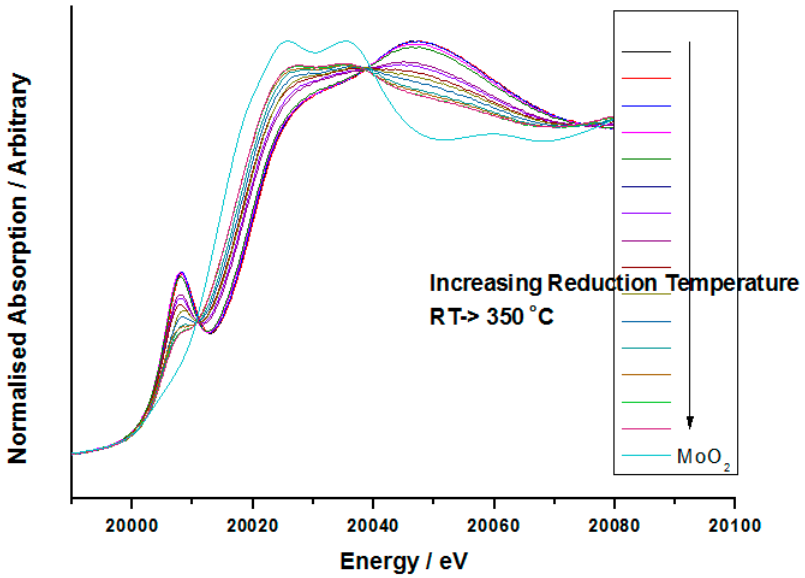

Figure 22. Temperature programmed XAS showing the reduction of 6ML MoO_x/Fe_2O_3 in MeOH/He while heating from ambient temperature to 350 °C, together with MoO_2 reference (pale blue). A shift in the absorption edge, to lower energy is seen with increasing temperature. Image adapted from C. Brookes et al., *Catal. Sci. Technol.*, 2016, 6, 722 [35].

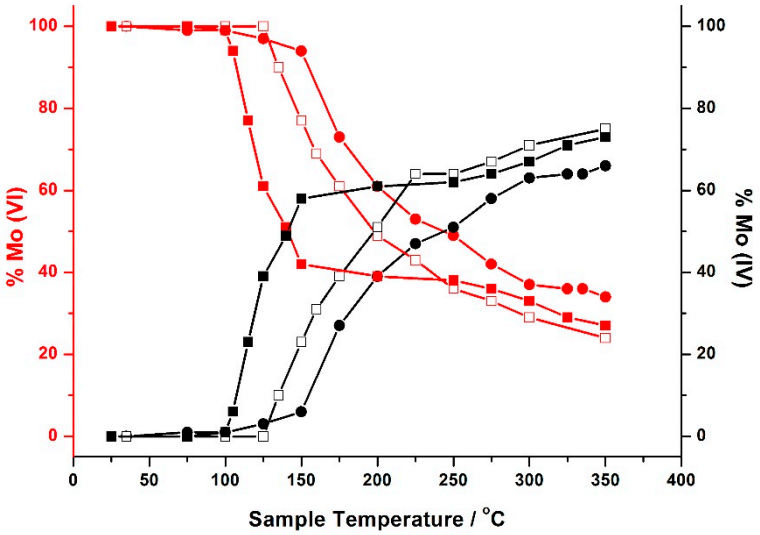

Figure 23. Oxidation state changes during in situ reduction of 1, 3 and 6ML MoO_x/Fe_2O_3 ascertained through monitoring the change in absorption edge position from Mo (VI) to Mo (IV). Reduction was carried out in a MeOH/He flow whilst heating to 350°C at a rate of 12 °C· min^{-1} under atmospheric pressure. XAFS spectra were collected throughout (~1 min per scan). 1ML = filled squares, 3ML = open squares, 6ML = filled circles. Figure adapted from C. Brookes et al., *Catal. Sci. Technol.*, 2016, 6, 722 [35].

This surface specific Mo–Mo bonded distance was an important finding, indicating the presence of a reduced cluster of Mo after reduction under MeOH/He. The significance of these Mo clusters is that the possible dimer unit could suggest a two centred Mo reaction site, which could be the reactive site that temporarily forms on reaction with methanol (the reductant) before its quick and efficient re-oxidation back to the original catalyst. This complements the results of Kikutani et al. [56] who found that a 2.6 Å Mo–Mo bond in fixed dimer catalysts as the most distinctive feature for unique dimeric active sites. This proposal is now recognized by many, with evidence highly favouring this dual site option. A study by Lopez et al. used density functional theory (DFT) to describe the unique character of the Mo (VI)–Mo (IV) pairs as the most active and selective sites on the surface, to establish the controlling factors of selectivity, and the role of dopants [57]. It has been suggested that iron reduces the energy requirements of the redox Mo (VI)–Mo (IV) pair by acting as an electron reservoir.

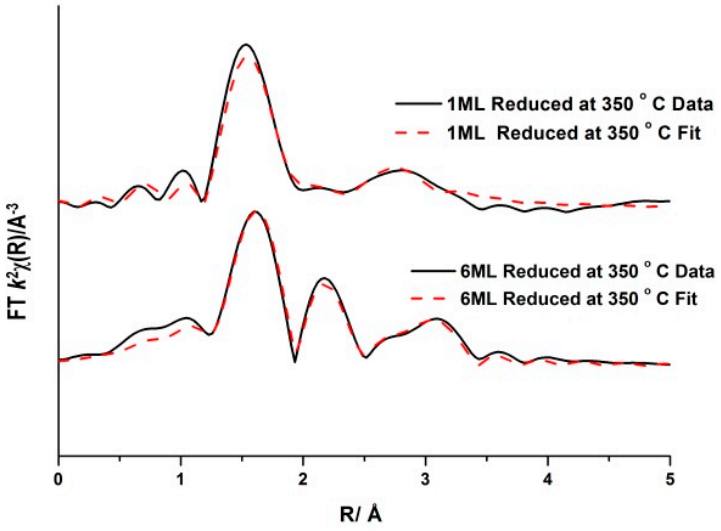

Figure 24. Magnitude component of the k^2-weighted Fourier Transform for the EXAFS data of the 1 and 6ML MoO_x/Fe_2O_3 catalyst reduced.

Table 3. EXAFS fitting parameters for the 1 and 6ML MoO_x/Fe_2O_3 reduced under MeOH/He at 350 °C. The R_{factor} for the 1 and 6ML reduced MoO_x/Fe_2O_3 catalysts were 0.03 and 0.01 respectively. Where, Abs. Sc. = Absorber-Scatterer atoms, N = Co-ordination number, *R* = Abs-Sc distance, $2\sigma^2$ = Amplitude reduction factor.

Sample	Abs. Sc.	N	*R*/Å	$2\sigma^2$/Å^2	E_f/eV	R_{factor}
1ML MoO_x/Fe_2O_3 end state *Reduced*	Mo–O	2 (2)	1.76 (5)	0.012 (1)	−1 (6)	0.03
	Mo–O	4.0 (1)	2.02 (2)	0.003 (Fixed)		
	Mo–Mo	1.3 (Fixed)	2.68 (3)	0.007 (2)		
	Mo–Fe	2 (2)	3.05 (6)	0.007 (Fixed)		
	Mo–Fe	2 (1)	3.36 (2)	0.007 (Fixed)		
6ML MoO_x/Fe_2O_3 end state *Reduced*	Mo–O	1.5 (1)	1.78 (2)	0.007 (7)	0 (2)	0.01
	Mo–O	3.4 (3)	2.03 (1)	0.003 (Fixed)		
	Mo–Mo	1.3 (Fixed)	2.62 (2)	0.003 (1)		
	Mo–Mo	2.5 (1)	2.82 (2)	0.01 (1)		
	Mo–Mo	4.0 (2)	3.37 (2)	0.01 (1)		

7. Investigating the Role of Fe in $Fe_2(MoO_4)_3$

The redox ability of molybdenum based catalysts has been discussed [8,37,58,59], with the oxidation state of the Mo considered a key contribution in catalyst reactivity. With extensive investigations into the role of Mo in the selective oxidation of methanol, the requirement for Fe in the active catalyst is still questioned, considering that it constitutes such a high proportion of the commercially-used catalyst.

There have been many theories postulated for the necessity of the iron containing phase [6,10,60]. Firstly it yields a catalyst with improved surface area, bringing increased overall activity in the oxidative reaction to formaldehyde. MoO_3 alone suffers from a very low surface area, therefore making it inappropriate for commercial use. Secondly, although it cannot compete with MoO_3, $Fe_2(MoO_4)_3$ demonstrates a satisfactory performance in the reaction to formaldehyde Moreover, $Fe_2(MoO_4)_3$ is thought to have superior properties such as its bulk lattice oxygen mobility, which allows the catalyst to always ensure sufficient oxygen regeneration to the surface during reaction, maintaining catalyst selectivity. The bulk reduction process of iron molybdate based catalysts has been investigated by Mössbauer [61] measurements on pure $Fe_2(MoO_4)_3$. The reduction takes place at temperatures above 230 °C, with the catalyst reducing to β-$FeMoO_4$. The process is shown to be completely reversible under oxygen at temperatures above 270 °C, with the catalyst efficiently reinstating its former $Fe_2(MoO_4)_3$ structure.

Further investigation into the properties in $Fe_2(MoO_4)_3$ have been addressed by the authors of this review, in an attempt to define the role of Fe in the industrially employed catalyst. MeOH pulsing studies have been executed under anaerobic conditions. Catalysts were subjected to continual MeOH pulsing, whilst being held isothermally at 350 °C under He. It was concluded that oxygen mobility at this temperature was enabled in $Fe_2(MoO_4)_3$, especially since the mixed oxide was able to maintain selectivity to formaldehyde for the duration of the experiment (Figure 25, Mass 30), though it also produced some CO (see Equation (7)). The presence of H_2CO was indicative of the presence of a methoxy intermediate at the surface. Methoxy has been proven to be present on MoO_3 [52,62].

$$CH_3OH + O_s \rightarrow H_2CO + H_2O \text{ Oxidative} \quad (6)$$

$$CH_3OH \rightarrow CO + 2H_2 \text{ Non} - \text{Oxidative} \quad (7)$$

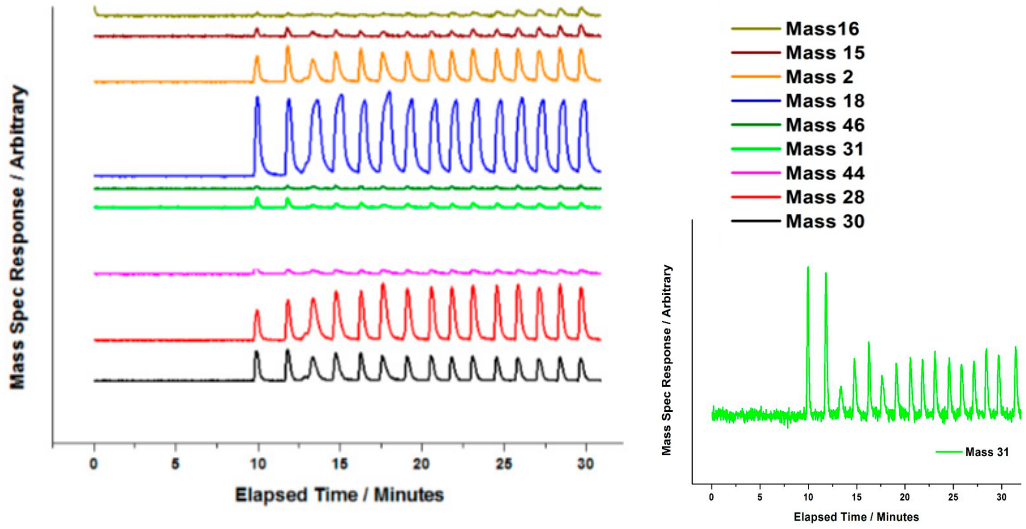

Figure 25. Pulse flow data for $Fe_2(MoO_4)_3$, Mo:Fe 1.5:1, under anaerobic conditions. MeOH pulsing was applied to the catalyst under He at 350 °C. The mass 31 data is expanded in the inset.

An equivalent pulsing experiment was performed on commercial MoO_3 (Figure 26). The catalyst was unable to match the performance of $Fe_2(MoO_4)_3$, with the conversion of methanol (Mass 31) occurring after approximately ten minutes into the pulsing regime, as opposed to the almost instant conversion for $Fe_2(MoO_4)_3$. The selectivity of formaldehyde was not maintained for the duration, with a significant drop in its production towards the end of the reaction. This is counterbalanced by an increase in CO production and conversion, which is not seen so quickly for $Fe_2(MoO_4)_3$. This suggests that bulk oxygen diffusion is hindered in MoO_3, causing significant reduction in the surface region (Equation (7)). Data suggests that $Fe_2(MoO_4)_3$ has properties other than simply providing an improved activity of the catalyst; it can also ameliorate the extent of this surface reduction. This corresponds well with other work in the literature [12,58,63]. A study by Ressler et al. [64] investigated the reduction of MoO_3 in propene, and the corresponding re-oxidation of MoO_2 by in situ X-ray diffraction (XRD) and X-ray absorption spectroscopy (XAS). The results revealed crucial information regarding solid-state kinetics of the processes, whilst also elucidating the structural changes occurring. It is believed that at temperatures below ~600 K, the contribution of oxygen from the MoO_3 bulk is negligible, leaving MoO_2 at the catalyst surface. A paper of Bowker et al. contrasts the behaviour of MoO_3 and MoO_2, with the latter showing an overall worse selectivity with a significantly higher proportion of CO produced [24]. It is not until 700 K that oxygen vacancy diffusion in the bulk is enough to allow for a slow-moving redox mechanism to occur. Above 700 K it is believed that fast oxygen diffusion permits the participation of a considerable amount of the lattice oxygen, and helps maintain the surface oxidation level for a longer period of time.

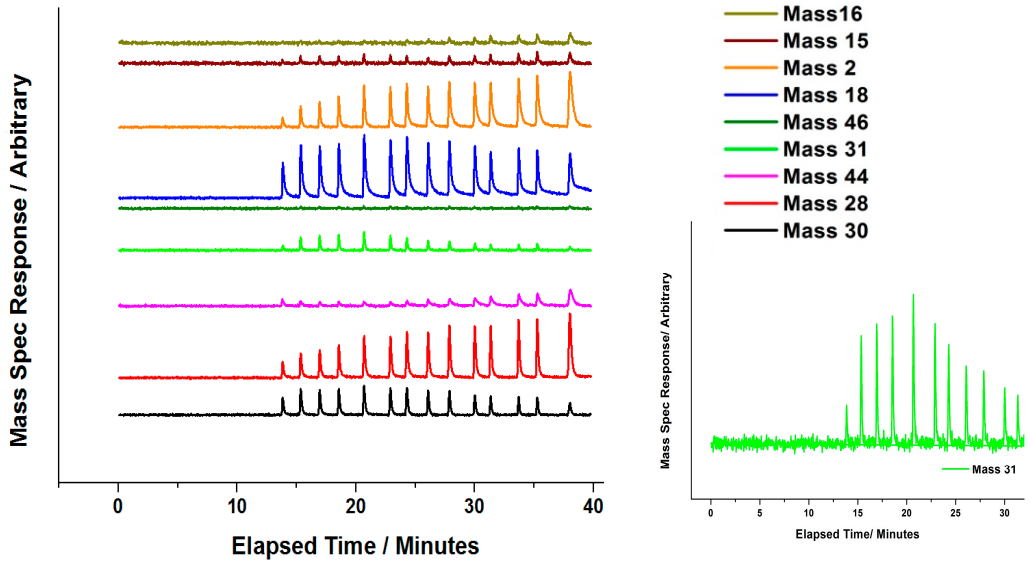

Figure 26. Pulsed flow data for MoO_3 under anaerobic conditions at 350 °C, experimental as Figure 25.

To elaborate further on this phenomenon, the oxygen lattice mobility has been investigated for $Fe_2(MoO_4)_3$ and MoO_3. It should be noted here that MoO_3 was produced in-house via precipitation, to produce the oxide with an equivalent surface area to that of $Fe_2(MoO_4)_3$. Although this area was difficult to maintain after one reaction cycle, it provided a means of fairly comparing the oxygen mobility in these two oxides (Figures 27 and 28). Following reduction in MeOH/He, catalysts were subjected to pulses of 10% O_2/He every 2 min at 350 °C. It was shown that for $Fe_2(MoO_4)_3$ (Figure 26), it was not until approximately 60 min into stage one of the pulsing regime, that the Mass 32 (oxygen) signal appeared. Oxygen saturation is not accomplished until 180 min, as shown through the consistency in peak area after this elapsed time. In an equivalent study on MoO_3, (Figure 28), a response for Mass 32 was seen after just 20 min into stage one of the pulsing regime, with a sharp rise from 40 min. The catalyst became fully saturated with oxygen after just 120 min, with no further uptake from this point. From these pulsing studies, it was revealed that $Fe_2(MoO_4)_3$ has a greater oxygen uptake than MoO_3, implying that the catalyst was more reduced under the same reduction regime. This therefore indicates a better redox activity of the catalyst. The study complements the reactivity data reported for the two catalysts (Figures 25 and 26).

TPPFR (Temperature Programmed Pulsed Flow Reaction) with MeOH/O_2 has also been indicative of surface oxygen removal. Bowker et al. [14,22] have demonstrated that surface oxygen is more readily removed from $Fe_2(MoO_4)_3$, established through the lowered temperature of conversion and formaldehyde production for this oxide The ease of reducibility has been shown by others to follow as: Fe_2O_3 > $Fe_2(MoO_4)_3$ > MoO_3 [65], suggesting that the mobility of the oxygen anions follows the same order, with the highest mobility in Fe_2O_3 and lowest in MoO_3. Not all agree however. Beale et al. [38] recently published a study involving a combined multi-technique in situ approach to probe the stability of $Fe_2(MoO_4)_3$ catalysts during redox cycling. According to these authors, the $Fe_2(MoO_4)_3$ phase is the primary active phase, and that during standard reaction, a partial reduction of this phase occurs, resulting in the formation of formaldehyde, inactive β-$FeMoO_4$ and MoO_3. The $FeMoO_4$ phase is short lived, and is rapidly re-oxidised back to $Fe_2(MoO_4)_3$ by gas phase oxygen. To probe this mechanism in more detail, the stoichiometric $Fe_2(MoO_4)_3$ catalyst has been studied in harsher anaerobic conditions, to accelerate the changes occurring. The catalyst was first reduced under MeOH/He, yielding formaldehyde. Post anaerobic treatment the catalyst was re-oxidised under air to monitor the ability of the catalyst to regenerate. In situ combined wide-angle X-ray scattering, X-ray absorption near edge spectroscopy and ultraviolet-visible spectroscopy with online mass spectrometry were combined to study the structure-activity relationships under redox cycling.

Under redox cycling, it was shown that the initial $Fe_2(MoO_4)_3$ is partially regenerated, however with subsequent re-oxidation, little regeneration occurs, and can only do after a long period of time.

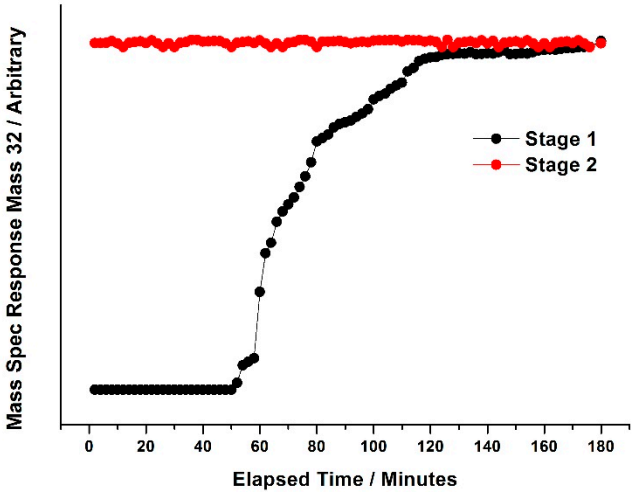

Figure 27. Oxygen pulsing study on reduced $Fe_2(MoO_4)_3$ at 350 °C, Stages 1–2. Post reductio, catalysts were subjected to pulses of 10% O_2/He from a known sample loop volume every two minutes. The uptake of oxygen was monitored through the change in peak integral of Mass 32. Each stage consisted of 180 min of pulsing. By stage two, 100% O_2 saturation had occurred.

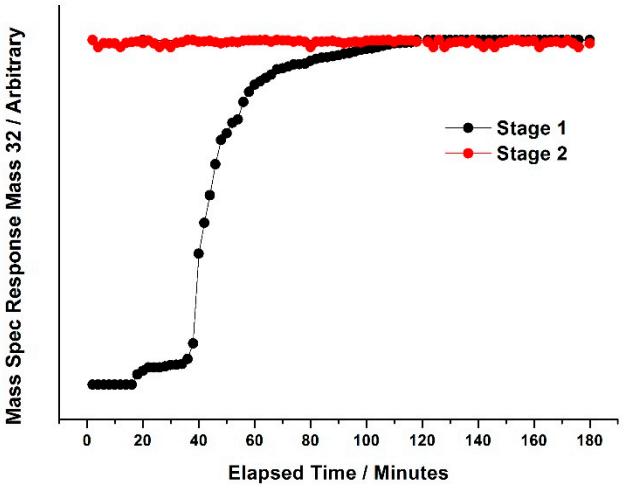

Figure 28. Oxygen pulsing study on reduced MoO_3 at 350 °C, Stages 1–2 (Studies as for $Fe_2(MoO_4)_3$ Figure 26).

8. Materials and Methods

8.1. Catalyst Synthesis

MoO_x/Fe_2O_3 catalysts were prepared by impregnating the desired number of ML equivalents of Mo oxide, through ammonium heptamolybdate, on commercial Fe_2O_3 (Sigma Aldrich, St. Louis, MO, USA, particle size <50 nm). A calcination of 500 °C for 3 h was employed for Fe_2O_3 in preparation for its use as a support. Aqueous ammonium heptamolybdate (for 3ML MoO_x/Fe_2O_3) was dosed onto the surface of the Fe_2O_3 by incipient wetness impregnation during constant mixing. Samples were subsequently dried at 120 °C for 24 h followed by annealing at different temperatures in air for 2 h.

Reference samples were prepared for comparison with the 3ML dosed materials. Iron molybdate (Mo/Fe ratio of 1.5:1) was prepared using a conventional coprecipitation method; a solution of iron

nitrate nonahydrate (Sigma Aldrich, >98%, St. Louis, MO, USA) was added dropwise to solution of ammonium heptamolybdate (Fluka Analytical, New York, NY, USA, >99%) previously acidified to pH 2 with dilute HNO_3, under continuous stirring. The mixture formed was then heated to 90 °C for approximately 1 h until a yellow sludge remained, which was air-dried overnight and then dried at 120 °C for 24 h, followed by calcination at 500 °C for 48 h.

8.2. Catalyst Characterisation

The morphology and homogeneity of the samples were determined by electron microscopy, with both TEM and SEM used. TEM ensured catalysts were homogeneous. Materials were examined using a model JEM 2100 EM (JEOL) and showed no discernable sign of particle clustering or agglomeration at the surface. SEM EDX analysis was performed using a JEOL model JSM-6610LV.

BET surface areas were determined under nitrogen physisorption at 77 K using a Micromeretics Gemini surface area analyzer (Micromeritics, Norcross, GA 30093, USA). Phase composition was assessed using a range of techniques, including vibrational spectroscopy. A Renishaw (Gloucetershire, UK) Raman microscope fitted with an 830 nm laser, was used to acquire Raman spectra. Measurements typically used a 0.1% laser power, with four accumulations at 10 s exposure time for each. A Panalytical X'pert pro analyzer with Cu Kα radiation was used for to perform XRD measurements.

An ESCALAB 220 spectrometer (VG Scientific, UK) equipped with AlKα and MgKα sources, and fitted with a fast entry lock for easy sample loading was used to acquire XPS spectra. AlKα (1486.6 eV) irradiation was used, to prevent Fe Auger peaks overlapping with the Fe 2p1/2 and Fe 2p3/2 peaks.

Mo K-edge XAFS studies were carried out at the UK national synchrotron, Diamond Light Source, on the B18 beamline (Rutherford Appleton Lab, Harwell, Oxfordshire, UK). Measurements used a double crystal Si (111) monochromator [66,67] for EXAFS in the range of 19,800 to 21,500 eV. All pellet (diluted with BN) samples of the as prepared materials and reference samples were collected in transmission mode. XAFS data processing and EXAFS analysis were performed using IFEFFIT with the Horae package (Athena and Artemis). The amplitude reduction factor, was derived from EXAFS data analysis of the known Mo reference compound, MoO_3, and determined as 0.82, and used fixed input parameter.

8.3. Catalyst Testing

A CATLAB reactor (Hiden Ltd., Warrington, UK) was used to assess the catalytic performance of the materials via TPD and continuous pulse flow studies. For the continuous pulse flow studies 1 μL of methanol was injected into a flow of 10% O_2/He every 2 min, at a flow rate of 30 mL min^{-1}. Products were determined by the online mass spectrometer. A temperature ramp of 12 °C min^{-1} was used during the studies. For TPD ~6 injections of 1 μL methanol were dosed onto the catalyst at room temperature in a flow of 30ML min? 1 of He. Subsequently the temperature was ramped to a maximum of 400 °C at a rate of 8 °C min^{-1}, monitoring the products of desorption through mass spectrometry.

9. Conclusions

The crucial factors which affect methanol selective oxidation on iron molybdate are the following. Firstly, the surface is entirely dominated by Mo oxide, and any presence of Fe in the surface layers of the catalyst are detrimental to selectivity. As a result, catalysts made by placing thin layers of Mo at the surface of iron oxide work very well (but not quite as well) as iron molybdate. Secondly the ability of the surface to display what we might call "structural redox flexibility" seems to be an important factor in such catalysis. What we mean by this is that the material must tolerate a degree of oxygen loss without permanent loss of structural integrity. This may be a reason for incorporating Fe into these materials, notwithstanding its total oxidation characteristics. It does not appear in the crucial surface layer, yet it enables easier subsurface diffusion of anion vacancies during oxygen starvation periods, and easy re-oxidation during surplus.

Acknowledgments: We thank the EPSRC for supporting the activities of the UK Catalysis Hub at RCaH (EP/I019693/1, EP/K014714/1). Thanks also go to Diamond Light Source and the Cardiff Catalysis Institute (CCI) for funding the studentship of Catherine Brookes. The authors thank Diamond Light Source for the allocation of beamtime (SP8071-1) and support of their staff. Thanks to Emma Gibson for the training and contributions towards the DRIFTS analysis.

Author Contributions: C.B. conducted the experiments, analysed the data and wrote this review. P.W. and M.B. directed the research strategy for the work, and reviewed the manuscript prior to submission.

Conflicts of Interest: The authors declare no conflict of interest.

Abbreviations

The following abbreviations are used in this manuscript:

acSTEM	Aberration Corrected Scanning Transmission Electron
BET	Brunauer, Emmett and Teller
DRIFTS	Diffuse Reflectance Infrared Fourier Transform Spectroscopy
EDX	Energy Dispersive X-rays
FTIR	Fourier Transform Infrared
HC	Hydrocarbon
LCA	Linear Combination Analysis
LCF's	Linear Combination Fitting's
ML	Monolayer
MVK	Mars-Van Krevelen
SEM	Scanning Electron Microscopy
TEM	Tranmission Electron Microscopy
TPD	Temperature Programme Desorption
TPPFR	Temperature Programmed Pulsed Flow Reaction
TPR	Temperature Programmed Reduction
WAXS	Wide-angle X-ray Scattering
XAFS	X-ray Absorption Fien Structure
XANES	X-ray Absorption Near Edge Structure
XAS	X-ray Absorption Spectroscopy
XPS	X-ray Photoelectron Spectroscopy
XRD	X-ray Diffraction

References

1. Kowatsch, S. Formaldehyde. In *Phenolic Resins: A Century of Progress*; Pilato, L., Ed.; Springer: Berlin/Heidelberg, Germany, 2010.
2. Adkins, H.; Peterson, W.R. The oxidation of methanol with air over iron, molybdenum, and iron-molybdenum oxides. *J. Am. Chem. Soc.* **1931**, *53*, 1512–1520. [CrossRef]
3. Soares, A.P.V.; Portela, M.F.; Kiennemann, A.; Hilaire, L. Mechanism of deactivation of iron-molybdate catalysts prepared by coprecipitation and sol-gel techniques in methanol to formaldehyde oxidation. *Chem. Eng. Sci.* **2003**, *58*, 1315–1322. [CrossRef]
4. Bowker, M.; Gibson, E.; Silverwood, I.P.; Brookes, C. Methanol oxidation on Fe_2O_3 catalysts and the effects of surface Mo. *Faraday Discuss.* **2015**. [CrossRef]
5. Routray, K.; Wachs, I.E. Role of excess MoO_3 in iron-molybdate methanol oxidation catalysts. *Abstr. Pap. Am. Chem. Soc.* **2007**, *233*.
6. Kim, T.H.; Ramachandra, B.; Choi, J.S.; Saidutta, M.; Choo, K.Y.; Song, S.-D.; Rhee, Y.-W. Selective oxidation of methanol to formaldehyde using modified iron-molybdate catalysts. *Catal. Lett.* **2004**, *98*, 161–165. [CrossRef]
7. Brookes, C.; Wells, P.P.; Dimitratos, N.; Jones, W.; Gibson, E.K.; Morgan, D.J.; Cibin, G.; Nicklin, C.; Mora-Fonz, D.; Scanlon, D.O.; et al. The nature of the molybdenum surface in iron molybdate. The active phase in selective methanol oxidation. *J. Phys. Chem. C* **2014**, *118*, 26155–26161. [CrossRef]
8. House, M.P.; Carley, A.F.; Echeverria-Valda, R.; Bowker, M. Effect of varying the cation ratio within iron molybdate catalysts for the selective oxidation of methanol. *J. Phys. Chem. C* **2008**, *112*, 4333–4341. [CrossRef]
9. Popov, B.; Shkuratova, L.; Orlova, L. Effect of excess molybdenum trioxide on the activity and selectivity of some molybdates in methanol oxidation. *React. Kinet. Catal. Lett.* **1976**, *4*, 323–328. [CrossRef]

10. Soares, A.V.; Portela, M.F.; Kiennemann, A.; Hilaire, L.; Millet, J. Iron molybdate catalysts for methanol to formaldehyde oxidation: Effects of Mo excess on catalytic behaviour. *Appl. Catal. A* **2001**, *206*, 221–229. [CrossRef]
11. Söderhjelm, E.; House, M.P.; Cruise, N.; Holmberg, J.; Bowker, M.; Bovin, J.-O.; Andersson, A. On the synergy effect in MoO_3–$Fe_2(MoO_4)_3$ catalysts for methanol oxidation to formaldehyde. *Top. Catal.* **2008**, *50*, 145–155. [CrossRef]
12. Routray, K.; Zhou, W.; Kiely, C.J.; Grünert, W.; Wachs, I.E. Origin of the synergistic interaction between MoO_3 and iron molybdate for the selective oxidation of methanol to formaldehyde. *J. Catal.* **2010**, *275*, 84–98. [CrossRef]
13. Volta, J.; Tatibouet, J. Structure sensitivity of MoO_3 in mild oxidation of propylene. *J. Catal.* **1985**, *93*, 467–470. [CrossRef]
14. Bowker, M.; Holroyd, R.; Elliott, A.; Morrall, P.; Alouche, A.; Entwistle, C.; Toerncrona, A. The selective oxidation of methanol to formaldehyde on iron molybdate catalysts and on component oxides. *Catal. Lett.* **2002**, *83*, 165–176. [CrossRef]
15. Routray, K. *Catalysis Science of Bulk Mixed Metal Oxides*; ProQuest: Ann Harbor, MI, USA, 2009.
16. Brookes, C.; Wells, P.P.; Cibin, G.; Dimitratos, N.; Jones, W.; Morgan, D.J.; Bowker, M. Molybdenum oxide on fe_2o_3 core-shell catalysts: Probing the nature of the structural motifs responsible for methanol oxidation catalysis. *ACS Catal.* **2013**, *4*, 243–250. [CrossRef]
17. House, M.P.; Shannon, M.D.; Bowker, M. Surface segregation in iron molybdate catalysts. *Catal. Lett.* **2008**, *122*, 210–213. [CrossRef]
18. Carbucicchio, M.; Trifiro, F. Surface and bulk redox processes in iron-molybdate-based catalysts. *J. Catal.* **1976**, *45*, 77–85. [CrossRef]
19. Okamoto, Y.; Morikawa, F.; Oh-Hiraki, K.; Imanaka, T.; Teranishi, S. Role of excess of MoO3 in Fe_2O_3–MoO_3 methanol oxidation catalysts studied by X-ray photoelectron spectroscopy. *J. Chem. Soc. Chem. Commun.* **1981**, 1018–1019. [CrossRef]
20. Bamroongwongdee, C.; Bowker, M.; Carley, A.F.; Davies, P.R.; Davies, R.J.; Edwards, D. Fabrication of complex model oxide catalysts: Mo oxide supported on Fe_3O_4 (111). *Faraday Discuss.* **2013**, *162*, 201–212. [CrossRef] [PubMed]
21. Popov, B.I.; Pashis, A.V.; Shkuratova, L.N. Effect of calcination temperature on the surface composition of Mo–Fe catalysts for methanol oxidation. *React. Kinet. Catal. Lett.* **1986**, *30*, 129–135. [CrossRef]
22. Bowker, M.; Holroyd, R.; House, M.; Bracey, R.; Bamroongwongdee, C.; Shannon, M.; Carley, A. The selective oxidation of methanol on iron molybdate catalysts. *Top. Catal.* **2008**, *48*, 158–165. [CrossRef]
23. Gai, P.L.; Labun, P.A. Electron microscopy studies relating to methanol oxidation over ferric molybdate and molybdenum trioxide catalysts. *J. Catal.* **1985**, *94*, 79–96. [CrossRef]
24. Bowker, M.; Carley, A.F.; House, M. Contrasting the behaviour of MoO_3 and MoO_2 for the oxidation of methanol. *Catal. Lett.* **2008**, *120*, 34–39. [CrossRef]
25. Langmuir, I. The adsorption of gases on plane surfaces of glass, mica and platinum. *J. Am. Chem. Soc.* **1918**, *40*, 1361–1403. [CrossRef]
26. Boreskov, G.; Kolovertnov, G.; Kefeli, L.; Plyasova, L.; Karakchiev, L.; Mastikhin, V.; Popov, V.; Dzis' Ko, V.; Tarasova, D. Study of an iron-molybdenum oxide catalyst for the oxidation of methanol to formaldehyde. II. Phase composition and nature of the catalytically active component. *Kinet. Catal. (Engl. Transl.)* **1965**, *7*, 125.
27. Bowker, M.; Brookes, C.; Carley, A.F.; House, M.P.; Kosif, M.; Sankar, G.; Wawata, I.; Wells, P.P.; Yaseneva, P. Evolution of active catalysts for the selective oxidative dehydrogenation of methanol on Fe_2O_3 surface doped with mo oxide. *Phys. Chem. Chem. Phys.* **2013**, *15*, 12056–12067. [CrossRef] [PubMed]
28. Busca, G.; Lamotte, J.; Lavalley, J.C.; Lorenzelli, V. FT-IR study of the adsorption and transformation of formaldehyde on oxide surfaces. *J. Am. Chem. Soc.* **1987**, *109*, 5197–5202. [CrossRef]
29. Hill, C.G.; Wilson, J.H. Raman spectroscopy of iron molybdate catalyst systems: Part I. Preparation of unsupported catalysts. *J. Mol. Catal.* **1990**, *63*, 65–94. [CrossRef]
30. Radhakrishnan, R.; Reed, C.; Oyama, S.T.; Seman, M.; Kondo, J.N.; Domen, K.; Ohminami, Y.; Asakura, K. Variability in the structure of supported MoO_3 catalysts: Studies using raman and X-ray absorption spectroscopy with ab initio calculations. *J. Phys. Chem. B* **2001**, *105*, 8519–8530. [CrossRef]

31. Xu, Y.; Spataro, B.; Sarti, S.; Dolgashev, V.A.; Tantawi, S.; Yeremian, A.D.; Higashi, Y.; Grimaldi, M.G.; Romano, L.; Ruffino, F.; et al. Structural and morphological characterization of Mo coatings for high gradient accelerating structures. In Proceedings of the 15th International Conference on X-ray Absorption Fine Structure (XAFS15), Beijing, China, 22–28 July 2012; Volume 430.
32. Hu, H.C.; Wachs, I.E.; Bare, S.R. Surface-structures of supported molybdenum oxide catalysts—Characterization by Raman and Mo L3-edge XANES. *J. Phys. Chem.* **1995**, *99*, 10897–10910. [CrossRef]
33. Ressler, T.; Timpe, O.; Neisius, T.; Find, J.; Mestl, G.; Dieterle, M.; Schlogl, R. Time-resolved XAS investigation of the reduction/oxidation of MoO_{3-x}. *J. Catal.* **2000**, *191*, 75–85. [CrossRef]
34. Huang, Y.; Cong, L.; Yu, J.; Eloy, P.; Ruiz, P. The surface evolution of a catalyst jointly influenced by thermal spreading and solid-state reaction: A case study with an Fe_2O_3–MoO_3 system. *J. Mol. Catal. A* **2009**, *302*, 48–53. [CrossRef]
35. Brookes, C.; Bowker, M.; Gibson, E.K.; Gianolio, D.; Mohammed, K.M.; Parry, S.; Rogers, S.M.; Silverwood, I.P.; Wells, P.P. In situ spectroscopic investigations of MoO_x/Fe_2O_3 catalysts for the selective oxidation of methanol. *Catal. Sci. Technol.* **2016**, *6*, 722–730. [CrossRef]
36. Bowker, M.; House, M.; Alshehri, A.; Brookes, C.; Gibson, E.; Wells, P.P. Selectivity determinants for dual function catalysts: applied to methanol selective oxidation on iron molybdate. *Catal. Struct. React.* **2015**, *1*, 95–100. [CrossRef]
37. O'Brien, M.G.; Beale, A.M.; Jacques, S.D.M.; Buslaps, T.; Honkimaki, V.; Weckhuysen, B.M. On the active oxygen in bulk MoO_3 during the anaerobic dehydrogenation of methanol. *J. Phys. Chem. C* **2009**, *113*, 4890–4897. [CrossRef]
38. O'Brien, M.G.; Beale, A.M.; Jacques, S.D.M.; Weckhuysen, B.M. A combined multi-technique in situ approach used to probe the stability of iron molybdate catalysts during redox cycling. *Top. Catal.* **2009**, *52*, 1400–1409. [CrossRef]
39. Pernicone, N.; Lazzerin, F.; Liberti, G.; Lanzavecchia, G. On the mechanism of CH_3OH oxidation to CH_2O over MoO_3Fe_2 $(MoO_4)_3$ catalyst. *J. Catal.* **1969**, *14*, 293–302. [CrossRef]
40. Doornkamp, C.; Ponec, V. The universal character of the mars and van krevelen mechanism. *J. Mol. Catal. A* **2000**, *162*, 19–32. [CrossRef]
41. House, M.P.; Carley, A.F.; Bowker, M. Selective oxidation of methanol on iron molybdate catalysts and the effects of surface reduction. *J. Catal.* **2007**, *252*, 88–96. [CrossRef]
42. Zhang, H.; Shen, J.; Ge, X. The reduction behavior of Fe–Mo–O catalysts studied by temperature-programmed reduction combined with in situ mössbauer spectroscopy and X-ray diffraction. *J. Solid State Chem.* **1995**, *117*, 127–135. [CrossRef]
43. Rodriguez, J.A.; Hanson, J.C.; Chaturvedi, S.; Maiti, A.; Brito, J.L. Studies on the behavior of mixed-metal oxides: Structural, electronic, and chemical properties of β-$FeMoO_4$. *J. Phys. Chem. B* **2000**, *104*, 8145–8152. [CrossRef]
44. Allison, J.N.; Goddard, W.A., III. Oxidative dehydrogenation of methanol to formaldehyde. *J. Catal.* **1985**, *92*, 127–135. [CrossRef]
45. Farneth, W.E.; Ohuchi, F.; Staley, R.H.; Chowdhry, U.; Sleight, A.W. Mechanism of partial oxidation of methanol over molybdenum(VI) oxide as studied by temperature-programmed desorption. *J. Phys. Chem.* **1985**, *89*, 2493–2497. [CrossRef]
46. Farneth, W.E.; McCarron, E.M.; Sleight, A.W.; Staley, R.H. A comparison of the surface chemistry of two polymorphic forms of molybdenum trioxide. *Langmuir* **1987**, *3*, 217–223. [CrossRef]
47. Tatibouet, J.M. Methanol oxidation as a catalytic surface probe. *Appl. Catal. A* **1997**, *148*, 213–252. [CrossRef]
48. Tatibouet, J.M. Acido-basicité et sensibilité à la structure de la réaction d'oxydation catalytique du méthanol sur α-mno_3 cristallisé. I: Sites acides. *C. R. Séances Acad. Sci.* **1983**, *297*, 703–708.
49. Tatibouët, J.M.; Germain, J.E. A structure-sensitive oxidation reaction: Methanol on molybdenum trioxide catalysts. *J. Catal.* **1981**, *72*, 375–378. [CrossRef]
50. Groff, R.P. An infrared study of methanol and ammonia adsorption on molybdenum trioxide. *J. Catal.* **1984**, *86*, 215–218. [CrossRef]
51. Wadayama, T.; Saito, T.; Suëtaka, W. Metastable surface species on moo_3 observed in methanol vapor at an elevated temperature with polarization modulation infrared spectroscopy. *Appl. Surf. Sci.* **1984**, *20*, 199–201. [CrossRef]

52. Chung, J.S.; Miranda, R.; Bennett, C.O. Mechanism of partial oxidation of methanol over MoO_3. *J. Catal.* **1988**, *114*, 398–410. [CrossRef]
53. Trifiro, F.; Centola, P.; Pasquon, I. The role of a metal-oxygen double bond in the activity of molybdates in oxidation reactions. *J. Catal.* **1968**, *10*, 86–88. [CrossRef]
54. Burcham, L.J.; Briand, L.E.; Wachs, I.E. Quantification of active sites for the determination of methanol oxidation turn-over frequencies using methanol chemisorption and in-situ infrared techniques. 1. Supported metal oxide catalysts. *Langmuir* **2001**, *17*, 6164–6174. [CrossRef]
55. Pernicone, N. Deactivation of Fe-Mo oxide catalyst in industrial plant and simulation tests on laboratory scale. *Catal. Today* **1991**, *11*, 85–91. [CrossRef]
56. Kikutani, Y. Structures of molybdenum silica catalysts reduced by ethanol, and their relations to catalytic oxidation reactions: I. Structure changes of Mo/SiO_2 with gradual reduction by ethanol. *J. Mol. Catal. A* **1999**, *142*, 247–263. [CrossRef]
57. Rellán-Piñeiro, M.; López, N. The active molybdenum oxide phase in the methanol oxidation to formaldehyde (formox process): A DFT study. *ChemSusChem* **2015**, *8*, 2231–2239. [CrossRef] [PubMed]
58. Jacques, S.D.M.; Leynaud, O.; Strusevich, D.; Beale, A.M.; Sankar, G.; Martin, C.M.; Barnes, P. Redox behavior of Fe–Mo–O catalysts studied by ultrarapid in situ diffraction. *Angew. Chem.* **2006**, *118*, 459–462. [CrossRef]
59. Carbucicchio, M.; Trifiro, F. Redox processes at the surfaces of $Fe_2O_3MoO_3/SiO_2$ catalysts. *J. Catal.* **1980**, *62*, 13–18. [CrossRef]
60. Pernicone, N. $MoO_3Fe_2(MoO_4)_3$ catalysts for methanol oxidation. *J. Less Common Met.* **1974**, *36*, 289–297. [CrossRef]
61. Carbucicchio, M.; Trifirò, F. Surface and bulk redox processes in iron-molybdate-based catalysts. *J. Catal.* **1976**, *45*, 77–85. [CrossRef]
62. Cheng, W.-H. Methanol and formaldehyde oxidation study over molybdenum oxide. *J. Catal.* **1996**, *158*, 477–485. [CrossRef]
63. Soares, A.P.V.; Portela, M.F.; Kiennemann, A. Methanol selective oxidation to formaldehyde over iron-molybdate catalysts. *Catal. Rev.* **2005**, *47*, 125–174. [CrossRef]
64. Ressler, T.; Wienold, J.; Jentoft, R.E.; Neisius, T. Bulk structural investigation of the reduction of MoO_3 with propene and the oxidation of MoO_2 with oxygen. *J. Catal.* **2002**, *210*, 67–83. [CrossRef]
65. Kuang, W.; Fan, Y.; Chen, Y. Structure and reactivity of ultrafine Fe–Mo oxide particles prepared by the sol-gel method. *Langmuir* **2000**, *16*, 5205–5208. [CrossRef]
66. Dent, A.J.; Cibin, G.; Ramos, S.; Parry, S.A.; Gianolio, D.; Smith, A.D.; Scott, S.M.; Varandas, L.; Patel, S.; Pearson, M.R.; et al. Performance of B18, the core EXAFS bending magnet beamline at diamond. In Proceedings of the 15th International Conference on X-ray Absorption Fine Structure (XAFS15), Beijing, China, 22–28 July 2012; Volume 430.
67. Dent, A.J.; Cibin, G.; Ramos, S.; Smith, A.D.; Scott, S.M.; Varandas, L.; Pearson, M.R.; Krumpa, N.A.; Jones, C.P.; Robbins, P.E. B18: A core XAS spectroscopy beamline for Diamond. In Proceedings of the 14th International Conference on X-ray Absorption Fine Structure (XAFS14), Camerino, Italy, 26–31 July 2009; Volume 190.